



Product Change Notification - SYST-260VQG746

Date:

27 May 2020

Product Category:

Power Management - PWM Controllers

Affected CPNs:**Notification subject:**

Data Sheet - MIC2127A - 75V, Synchronous Buck Controller Featuring Adaptive

Notification text:

SYST-260VQG746

Microchip has released a new Product Documents for the MIC2127A - 75V, Synchronous Buck Controller Featuring Adaptive of devices. If you are using one of these devices please read the document located at [MIC2127A - 75V, Synchronous Buck Controller Featuring Adaptive](#).

Notification Status: Final**Description of Change:** The following is the list of modifications:

- 1) Updated content in the Features section
- 2) Updated the Typical Application circuit
- 3) Updated content in the Electrical Characteristics table.
- 4) Updated content in Section 2.0, Typical Characteristics Curves.
- 5) Updated content in Section 4.3, Current limit (ILIM)
- 6) Updated content in Section 4.5, High- Side MOSFET Gate Drive (DH)
- 7) Updated content in Section 5.0, Applications Information

Impacts to Data Sheet: None**Reason for Change:** To Improve Productivity**Change Implementation Status:** Complete**Date Document Changes Effective:** 27 May 2020

NOTE: Please be advised that this is a change to the document only the product has not been changed.

Markings to Distinguish Revised from Unrevised Devices: N/A**Attachment(s):**

[MIC2127A - 75V, Synchronous Buck Controller Featuring Adaptive](#)

Please contact your local [Microchip sales office](#) with questions or concerns regarding this notification.

Terms and Conditions:

If you wish to [receive Microchip PCNs via email](#) please register for our PCN email service at our [PCN home page](#) select register then fill in the required fields. You will find instructions about registering for Microchips PCN email service in the [PCN FAQ](#) section.

If you wish to [change your PCN profile, including opt out](#), please go to the [PCN home page](#) select login and sign into your myMicrochip account. Select a profile option from the left navigation bar and make the applicable selections.

Affected Catalog Part Numbers (CPN)

MIC2127AYML-T5

MIC2127AYML-TR

MIC2127AYML-TRVAO

75V, Synchronous Buck Controller Featuring Adaptive On-Time Control

Features

- Hyper Speed Control[®] Architecture Enables:
 - High input to output voltage conversion ratio capability
 - Any Capacitor[™] stable
 - Ultra-fast load transient response
- Wide 4.5V-75V Input Voltage Range
- Adjustable Output Voltage from 0.6V to 30V
- 270 kHz-800 kHz Programmable Switching Frequency
- Built-In 5V Regulator for Single-Supply Operation
- Auxiliary Bootstrap LDO for Improving System Efficiency
- Internal Bootstrap Diode
- Selectable Light Load Operating Mode
- Enable Input and Power Good Output
- Programmable Current Limit
- Hiccup Mode Short-Circuit Protection
- Soft Start, Internal Compensation and Thermal Shutdown
- Supports Safe Start-Up into a Prebiased Output
- **AEC-Q100 Qualified (VAO suffix)**

Applications

- Networking/Telecom Equipment
- Base Station, Servers
- Distributed Power Systems
- Industrial Power Supplies
- Automotive Power Supplies

General Description

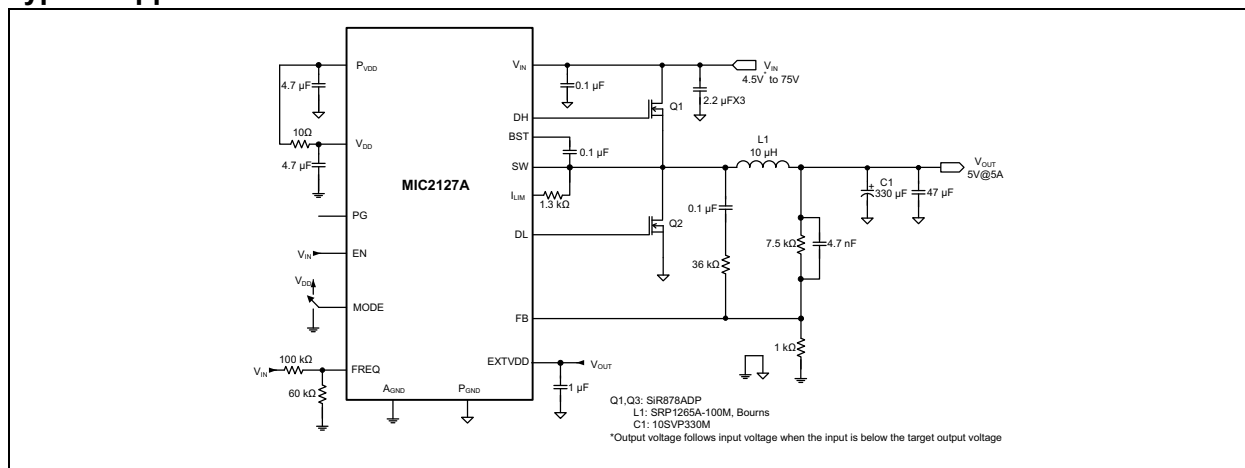
The MIC2127A device is a constant-frequency synchronous buck controller featuring a unique adaptive on-time control architecture. The MIC2127A device operates over an input voltage range from 4.5V-75V. The output voltage is adjustable down to 0.6V with an accuracy of $\pm 1\%$. The device operates with programmable switching frequency from 270 kHz to 800 kHz.

The MIC2127A device features a MODE pin that allows the user to select either Continuous Conduction mode or HyperLight Load[®] (HLL) mode under light loads. An auxiliary bootstrap LDO improves the system efficiency by supplying the MIC2127A internal circuit bias power and gate drivers from the output of the converter. A logic level enable (EN) signal can be used to enable or disable the controller. MIC2127A can start-up monotonically into a prebiased output. The MIC2127A device features an open drain power good signal (PG) that signals when the output is in regulation and can be used for simple power supply sequencing.

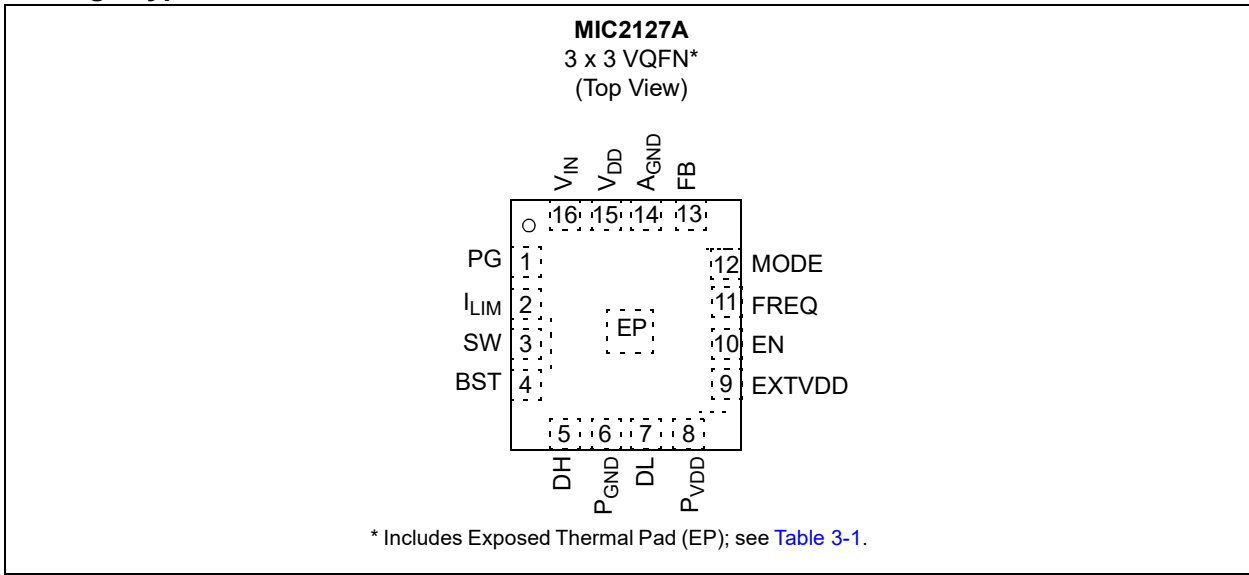
MIC2127A offers a full suite of protection features to ensure protection of the IC during Fault conditions. These include undervoltage lockout to ensure proper operation under power-sag conditions, "hiccup" mode short-circuit protection, internal soft start of 5 ms to reduce inrush current during start-up and thermal shut-down.

The MIC2127A device is available in a 16-pin 3 mm × 3 mm VQFN package, with an operating junction temperature range from -40°C to $+125^{\circ}\text{C}$.

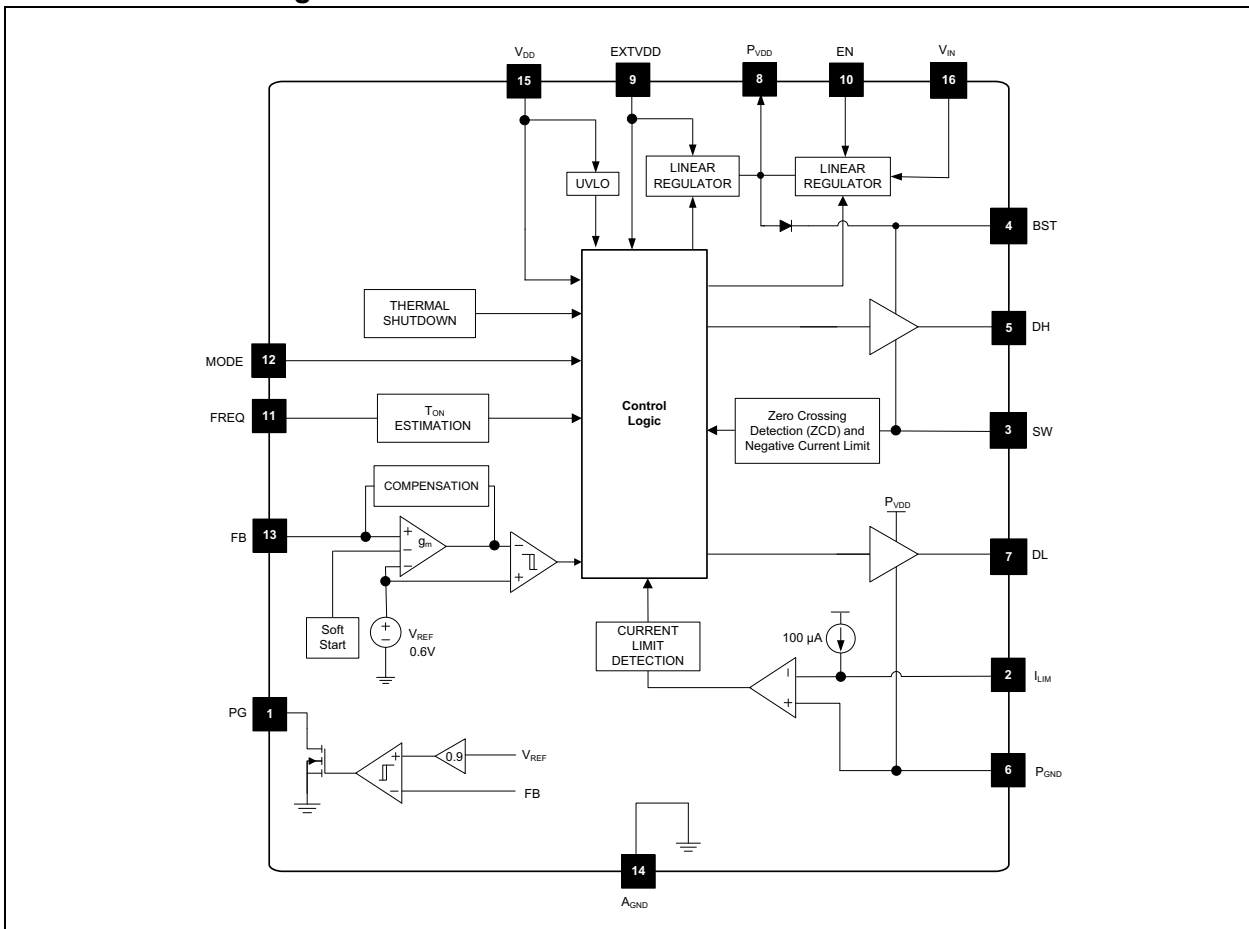
Typical Application Circuit



Package Type



Functional Block Diagram



1.0 ELECTRICAL CHARACTERISTICS

Absolute Maximum Ratings †

V_{IN} , FREQ, I_{LIM} , SW to P_{GND}	-0.3V to +76V
V_{SW} to P_{GND} (Transient < 50 ns)	-5V
V_{DD} , P_{VDD} , FB, PG, MODE to A_{GND}	-0.3V to +6V
EXTVDD to A_{GND}	-0.3V to +16V
BST to SW	-0.3V to +6V
BST to A_{GND}	-0.3V to +82V
EN to A_{GND}	-0.3V to (V_{IN} +0.3V)
DH, DL to A_{GND}	-0.3V to (V_{DD} +0.3V)
P_{GND} to A_{GND}	-0.3V to +0.3V
Junction Temperature	+150°C
Storage Temperature (T_S)	-65°C to +150°C
Lead Temperature (soldering, 10s)	260°C
ESD Rating ⁽¹⁾	1000V

† **Notice:** Stresses above those listed under “Maximum Ratings” may cause permanent damage to the device. This is a stress rating only and functional operation of the device at those or any other conditions above those indicated in the operational sections of this specification is not intended. Exposure to maximum rating conditions for extended periods may affect device reliability.

Note 1: Devices are ESD sensitive. Handling precautions recommended. Human body model, 1.5 k Ω in series with 100 pF.

Operating Ratings⁽¹⁾

Supply Voltage (V_{IN})	4.5V to 75V
SW, FREQ, I_{LIM} , EN	0V to V_{IN}
EXTVDD	0V to 13.2V
Junction Temperature (T_J)	-40°C to +125°C
Package Thermal Resistance (3 mm \times 3 mm VQFN 16LD)	
Junction-to-Ambient (θ_{JA})	50.8°C/W
Junction-to-Case (θ_{JC})	25.3°C/W

Note 1: The device is not ensured to function outside the operating range.

ELECTRICAL CHARACTERISTICS (Note 1)

Electrical Specifications: unless otherwise specified, $V_{IN} = 12V$, $V_{OUT} = 1.2V$; $V_{BST} - V_{SW} = 5V$, $T_A = +25^\circ C$. **Boldface** values indicate $-40^\circ C \leq T_J \leq +125^\circ C$ (Note 4)

Parameter	Symbol	Min.	Typ.	Max.	Units	Test Conditions
Power Supply Input						
Input Voltage Range (Note 2)	V_{VIN}	4.5	—	5.5	V	P_{VDD} and V_{DD} shorted to V_{IN} ($V_{PVDD} = V_{VIN} = V_{VDD}$)
		5.5	—	75		
Quiescent Supply Current	I_Q	—	1.4	1.8	mA	$V_{FB} = 1.5V$, $MODE = V_{DD}$, no switching
		—	300	600	μA	$V_{FB} = 1.5V$, $MODE = A_{GND}$, no switching
Shutdown Supply Current	$I_{VIN(SHDN)}$	—	0.1	5	μA	EN = Low
		—	30	60	μA	EN = Low, $V_{IN} = V_{DD} = 5.5V$
P_{VDD}, V_{DD} and EXTV_{DD}						
P_{VDD} Output Voltage	V_{PVDD}	4.8	5.1	5.4	V	$V_{VIN} = 7V$ to $75V$, $I_{PVDD} = 10$ mA
V_{DD} UVLO Threshold	$V_{VDD_UVLO_Rise}$	3.7	4.2	4.5	V	V_{DD} rising
V_{DD} UVLO Hysteresis	$V_{VDD_UVLO_Hys}$	—	600	—	mV	V_{DD} falling (Note 5)
EXT V_{DD} Bypass Threshold	V_{EXTVDD_Rise}	4.4	4.6	4.85	V	EXT V_{DD} rising
EXT V_{DD} Bypass Hysteresis	V_{EXTVDD_Hys}	—	200	—	mV	—
EXT V_{DD} Dropout Voltage	—	—	250	—	mV	$V_{EXTVDD} = 5V$, $I_{PVDD} = 25$ mA
Reference						
Feedback Reference Voltage	V_{REF}	0.597	0.6	0.603	V	$T_J = 25^\circ C$
		0.594	0.6	0.606	V	$-40^\circ C \leq T_J \leq 125^\circ C$
FB Bias Current (Note 3)	I_{FB}	—	50	500	nA	$V_{FB} = 0.6V$
Enable Control						
EN Logic Level High	V_{EN_H}	1.6	—	—	V	—
EN Logic Level Low	V_{EN_L}	—	—	0.6	V	—
EN Hysteresis	V_{EN_Hys}	—	100	—	mV	Note 5
EN Bias Current	I_{EN}	—	6	30	μA	$V_{EN} = 12V$
ON Timer						
Switching Frequency	f_{SW}	—	800	—	kHz	$V_{FREQ} = V_{VIN}$, $V_{VIN} = 12V$ $V_{FREQ} = 33\%$ of V_{VIN} , $V_{VIN} = 12V$
		230	270	300		
Maximum Duty Cycle	D_{MAX}	—	85	—	%	$V_{FREQ} = V_{VIN} = 12V$
Minimum Duty Cycle	D_{MIN}	—	0	—	%	$V_{FB} > 0.6V$ (Note 5)
Minimum ON Time	$t_{ON(MIN)}$	—	80	—	ns	—
Minimum OFF Time	$t_{OFF(MIN)}$	150	230	350	ns	—

Note 1: Specification for packaged product only.

2: The application is fully functional at low V_{DD} (supply of the control section) if the external MOSFETs have low voltage V_{TH} .

3: Design specification.

4: Temperature limits apply for automotive AEC-Q100 qualified part.

5: Not production tested.

ELECTRICAL CHARACTERISTICS

Electrical Specifications: unless otherwise specified, $V_{IN} = 12V$, $V_{OUT} = 1.2V$; $V_{BST} - V_{SW} = 5V$, $T_A = +25^\circ C$. **Boldface** values indicate $-40^\circ C \leq T_J \leq +125^\circ C$ (**Note 4**)

Parameter	Symbol	Min.	Typ.	Max.	Units	Test Conditions
MODE						
MODE Logic High Level	V_{MODE_H}	1.6	—	—	V	—
MODE Logic Low Level	V_{MODE_L}	—	—	0.6	V	—
MODE Hysteresis	V_{MODE_Hys}	—	70	—	mV	Note 5
Current Limit						
Current Limit Comparator Offset	V_{OFFSET}	-15	0	15	mV	$V_{FB} = 0.59V$
I_{LIM} Source Current	I_{CL}	85	100	115	μA	$V_{FB} = 0.59V$
I_{LIM} Source Current Tempco	TC_{ICL}	—	0.3	—	$\mu A/^\circ C$	Note 5
Negative Current Limit Comparator Threshold	V_{NCLTH}	—	48	—	mV	—
Zero Crossing Detection Comparator						
Zero Crossing Detection Comparator Threshold	V_{ZCDTH}	-15	-8	10	mV	—
FET Drivers						
DH On-Resistance, High State	$R_{DH(PULL_UP)}$	—	2	3	Ω	—
DH On-Resistance, Low State	$R_{DH(PULL_DOWN)}$	—	2	4	Ω	—
DL On-Resistance, High State	$R_{DL(PULL_UP)}$	—	2	4	Ω	—
DL On-Resistance, Low State	$R_{DL(PULL_DOWN)}$	—	0.36	0.8	Ω	—
SW, VIN, and BST Leakage						
BST Leakage	$I_{LK(BST)}$	—	—	30	μA	—
V_{IN} Leakage	$I_{LK(VIN)}$	—	—	50	μA	—
SW Leakage	$I_{LK(SW)}$	—	—	50	μA	—
Power Good (PG)						
PG Threshold Voltage	V_{PG_Rise}	85	—	95	$\%V_{OUT}$	V_{FB} rising
PG Hysteresis	V_{PG_Hys}	—	6	—	$\%V_{OUT}$	V_{FB} falling
PG Delay Time	PG_R_DLY	—	150	—	μs	V_{FB} rising
PG Low Voltage	V_{OL_PG}	—	140	200	mV	$V_{FB} < 90\% \times V_{NOM}$, $I_{PG} = 1\text{ mA}$
Thermal Protection						
Overtemperature Shutdown	T_{SHDN}	—	150	—	$^\circ C$	Junction temperature rising
Overtemperature Shutdown Hysteresis	T_{SHDN_Hys}	—	15	—	$^\circ C$	—

Note 1: Specification for packaged product only.

2: The application is fully functional at low V_{DD} (supply of the control section) if the external MOSFETs have low voltage V_{TH} .

3: Design specification.

4: Temperature limits apply for automotive AEC-Q100 qualified part.

5: Not production tested.

TEMPERATURE SPECIFICATIONS

Parameters	Sym.	Min.	Typ.	Max.	Units	Conditions	
Temperature Ranges							
Operating Junction Temperature	T_J	-40	—	+125	°C	Note 1	
Maximum Junction Temperature	$T_{J(MAX)}$	—	—	+150	°C	—	
Storage Temperature	T_S	-65	—	+150	°C	—	
Lead Temperature	T_{LEAD}	—	—	+260	°C	Soldering, 10s	
Package Thermal Resistances							
Thermal Resistance, 16 Lead, 3 x 3 mm VQFN	Junction-to-Ambient	θ_{JA}	—	50.8	—	°C/W	—
	Junction-to-Case	θ_{JC}	—	25.3	—	°C/W	—

Note 1: The maximum allowable power dissipation is a function of ambient temperature, the maximum allowable junction temperature and the thermal resistance from junction-to-air (i.e., T_A , T_J , θ_{JA}). Exceeding the maximum allowable power dissipation will cause the device operating junction temperature to exceed the maximum +125°C rating. Sustained junction temperatures above +125°C can impact the device reliability.

2.0 TYPICAL CHARACTERISTIC CURVES

Note: The graphs and tables provided following this note are a statistical summary based on a limited number of samples and are provided for informational purposes only. The performance characteristics listed herein are not tested or guaranteed. In some graphs or tables, the data presented may be outside the specified operating range (e.g., outside specified power supply range) and therefore outside the warranted range.

Note: Unless otherwise indicated, $V_{VIN} = 12V$, $f_{SW} = 300\text{ kHz}$, $R_{CL} = 1.3\text{ k}\Omega$, $L = 10\text{ }\mu\text{H}$, $V_{EXTVDD} = V_{OUT}$, $T_A = +25^\circ\text{C}$ (refer to the [Typical Application Circuit](#) circuit).

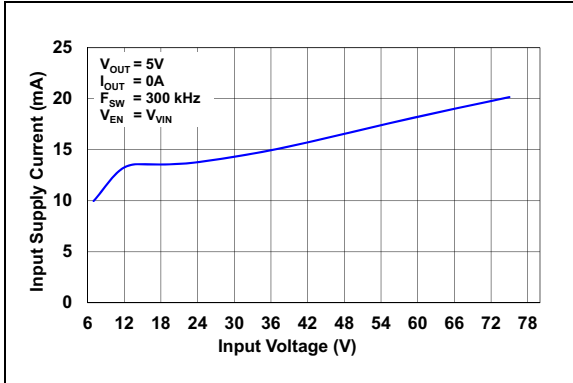


FIGURE 2-1: Input Supply Current vs. Input Voltage.

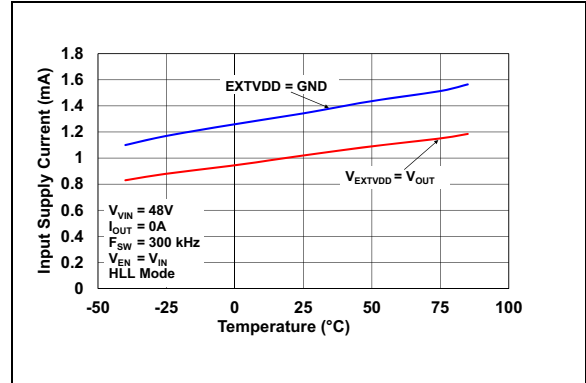


FIGURE 2-4: Input Supply Current vs. Temperature (HLL Mode).

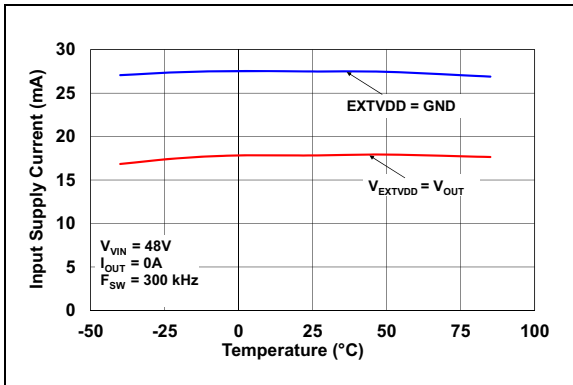


FIGURE 2-2: Input Supply Current vs. Temperature.

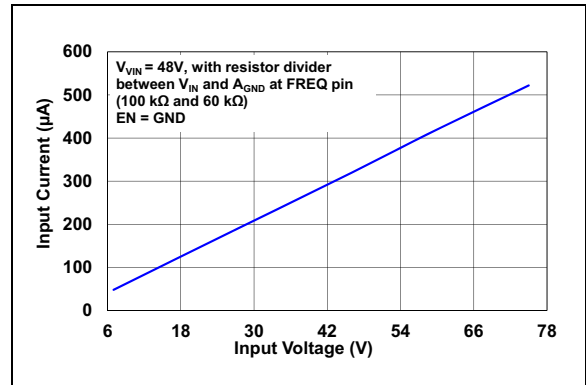


FIGURE 2-5: Input Shutdown Current vs. Input Voltage.

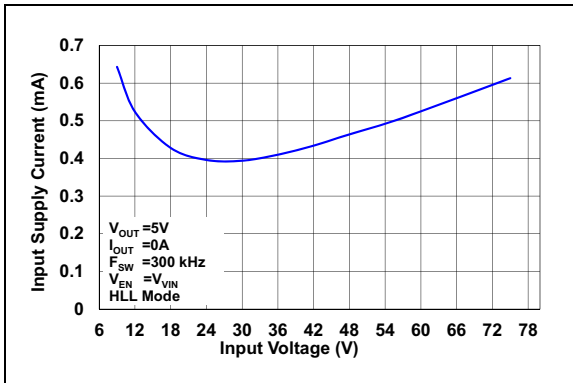


FIGURE 2-3: Input Supply Current vs. Input Voltage (HLL Mode).

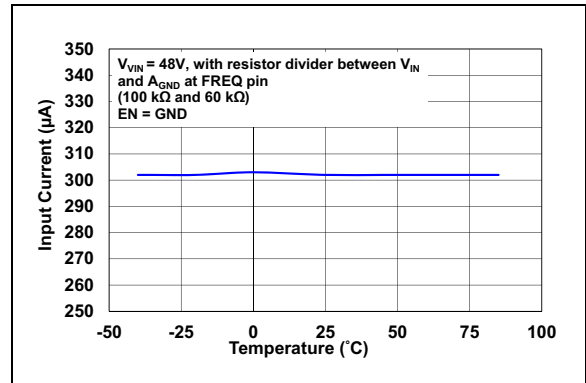


FIGURE 2-6: Input Shutdown Current vs. Temperature.

Note: Unless otherwise indicated, $V_{VIN} = 12V$, $f_{SW} = 300\text{ kHz}$, $R_{CL} = 1.3\text{ k}\Omega$, $L = 10\text{ }\mu\text{H}$, $V_{EXTVDD} = V_{OUT}$, $T_A = +25^\circ\text{C}$ (refer to the [Typical Application Circuit](#) circuit).

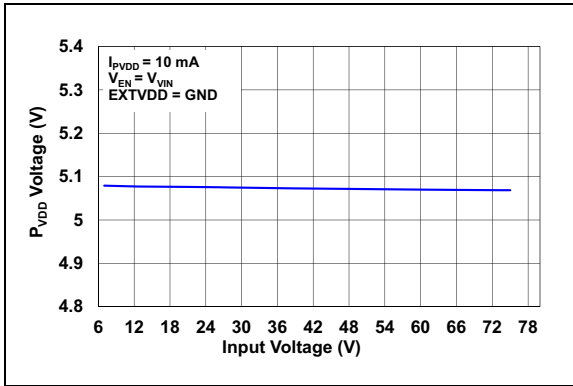


FIGURE 2-7: P_{VDD} Line Regulation.

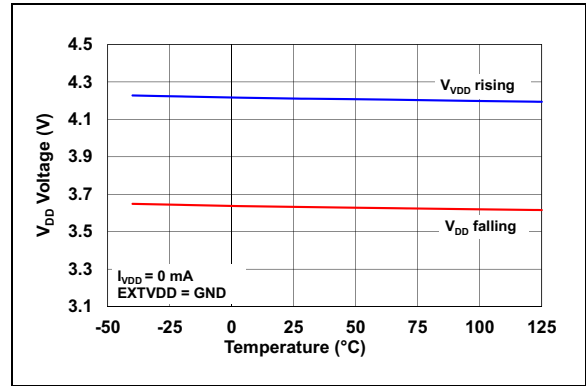


FIGURE 2-10: V_{DD} UVLO Threshold vs. Temperature.

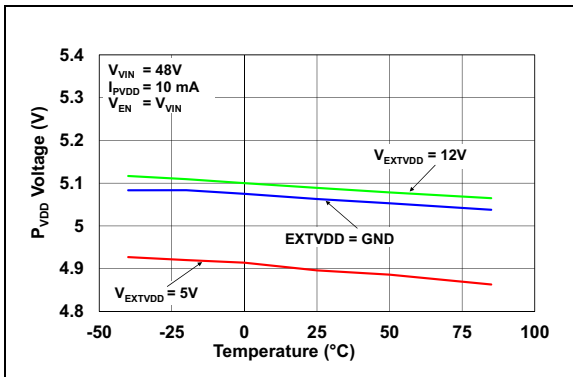


FIGURE 2-8: P_{VDD} Voltage vs. Temperature.

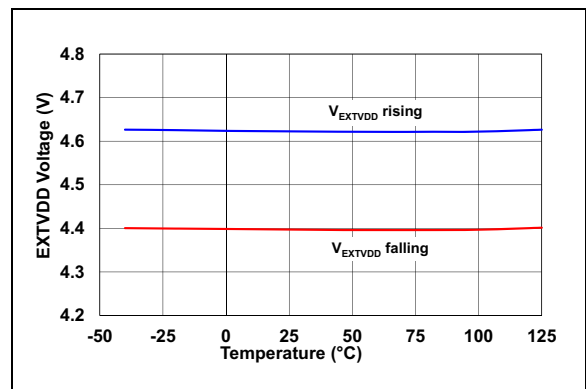


FIGURE 2-11: EXT_{VDD} Threshold vs. Temperature.

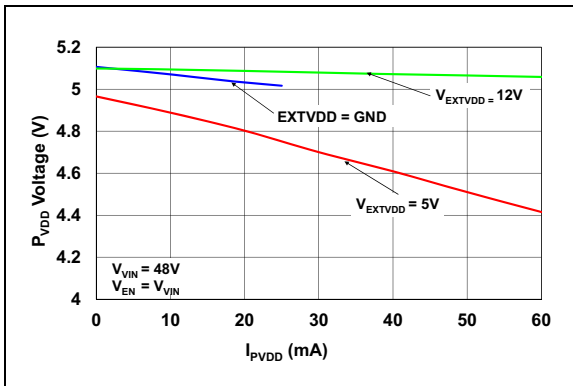


FIGURE 2-9: P_{VDD} Load Regulation.

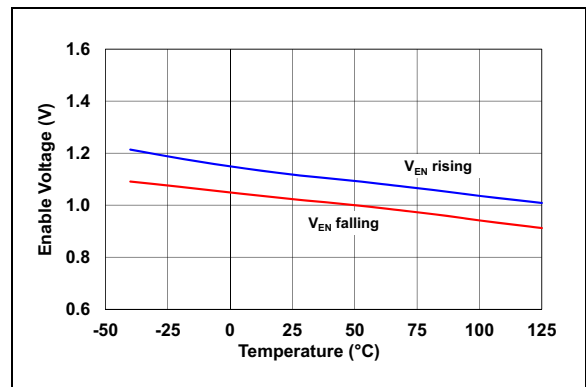


FIGURE 2-12: Enable Threshold vs. Temperature.

Note: Unless otherwise indicated, $V_{VIN} = 12V$, $f_{SW} = 300\text{ kHz}$, $R_{CL} = 1.3\text{ k}\Omega$, $L = 10\text{ }\mu\text{H}$, $V_{EXTVDD} = V_{OUT}$, $T_A = +25^\circ\text{C}$ (refer to the [Typical Application Circuit](#) circuit).

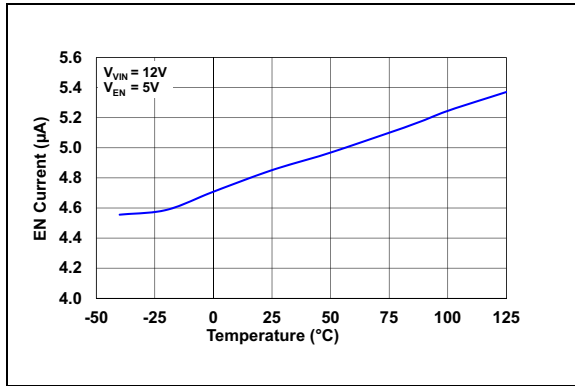


FIGURE 2-13: Enable Bias Current vs. Temperature.

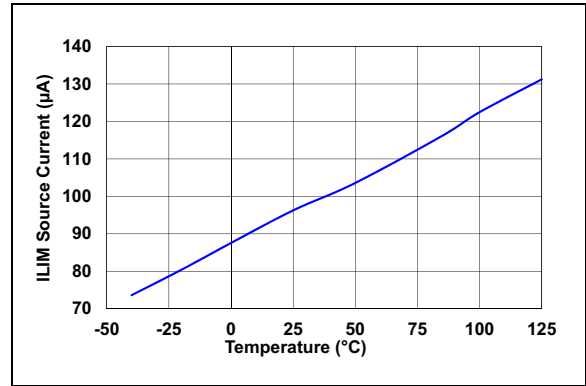


FIGURE 2-16: I_{LIM} Source Current vs. Temperature.

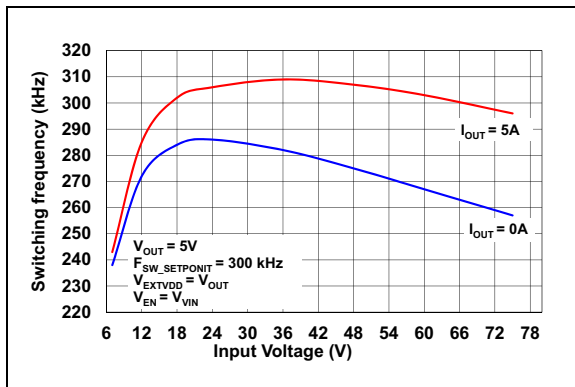


FIGURE 2-14: Switching Frequency vs. Input Voltage.

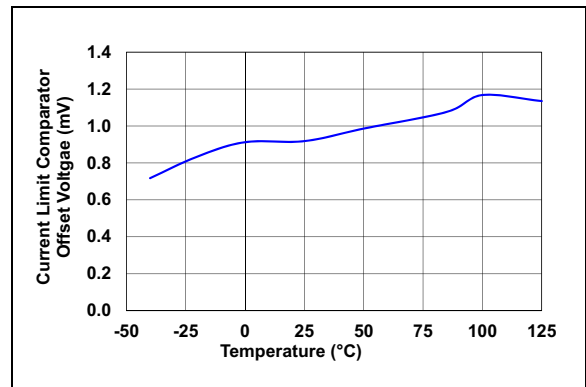


FIGURE 2-17: Current Limit Comparator Offset vs Temperature.

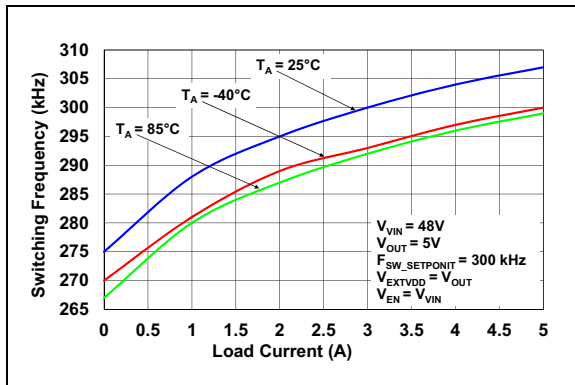


FIGURE 2-15: Switching Frequency vs. Load Current.

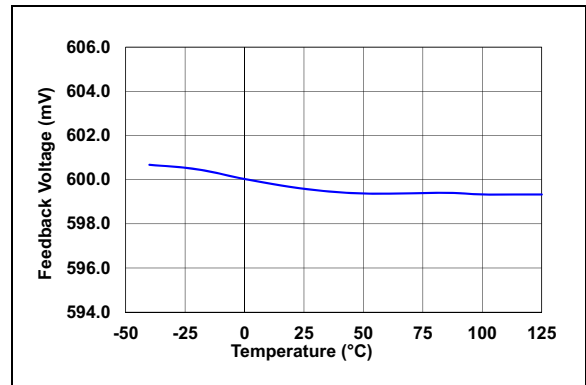


FIGURE 2-18: Feedback Voltage vs. Temperature.

Note: Unless otherwise indicated, $V_{VIN} = 12V$, $f_{SW} = 300\text{ kHz}$, $R_{CL} = 1.3\text{ k}\Omega$, $L = 10\text{ }\mu\text{H}$, $V_{EXTVDD} = V_{OUT}$, $T_A = +25^\circ\text{C}$ (refer to the [Typical Application Circuit](#) circuit).

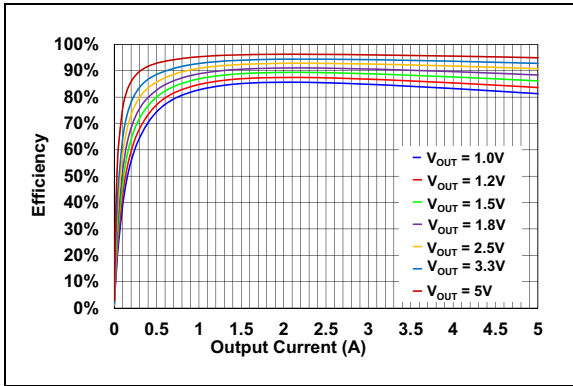


FIGURE 2-19: Efficiency vs. Output Current (Input Voltage = 12V, CCM Mode).

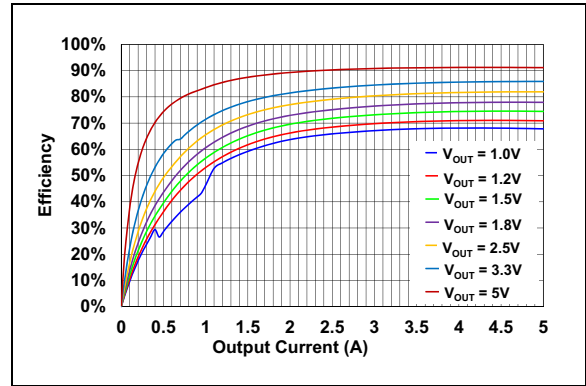


FIGURE 2-22: Efficiency vs. Output Current (Input Voltage = 48V, CCM Mode).

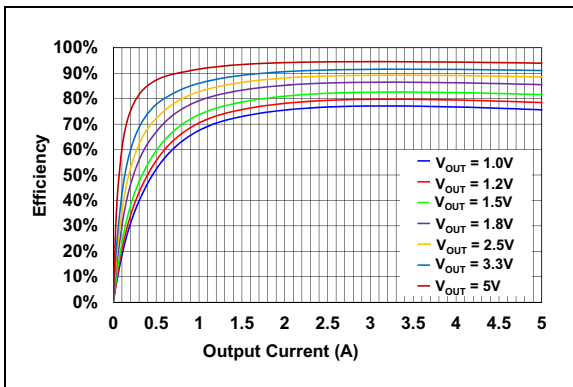


FIGURE 2-20: Efficiency vs. Output Current (Input Voltage = 24V, CCM Mode).

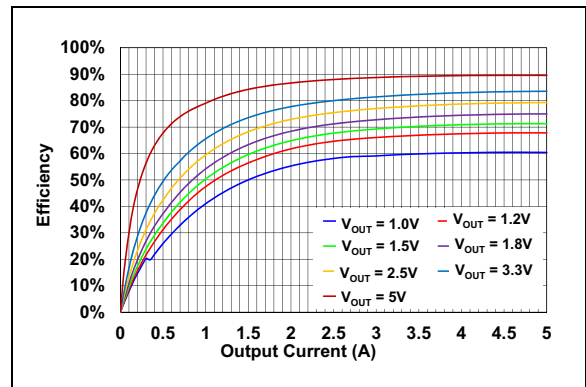


FIGURE 2-23: Efficiency vs. Output Current (Input Voltage = 60V, CCM Mode).

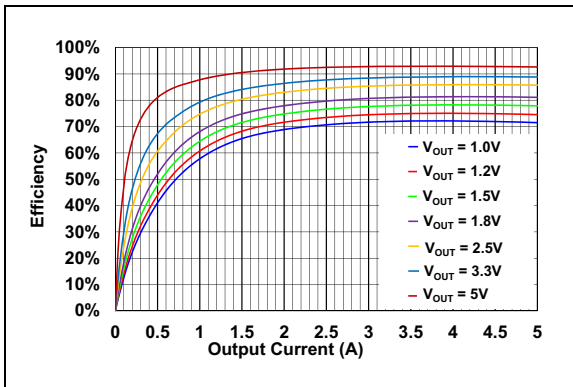


FIGURE 2-21: Efficiency vs. Output Current (Input Voltage = 36V, CCM Mode).

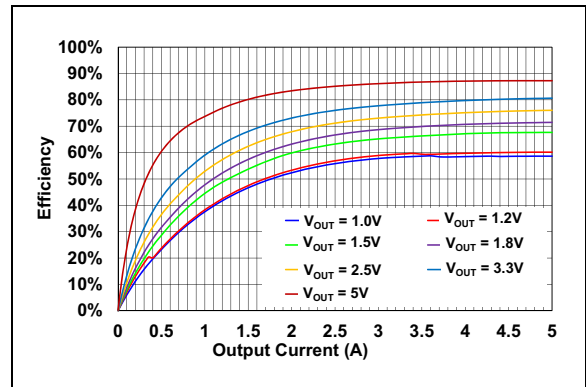


FIGURE 2-24: Efficiency vs. Output Current (Input Voltage = 75V, CCM Mode).

Note: Unless otherwise indicated, $V_{IN} = 12V$, $f_{SW} = 300\text{ kHz}$, $R_{CL} = 1.3\text{ k}\Omega$, $L = 10\text{ }\mu\text{H}$, $V_{EXTVDD} = V_{OUT}$, $T_A = +25^\circ\text{C}$ (refer to the [Typical Application Circuit](#) circuit).

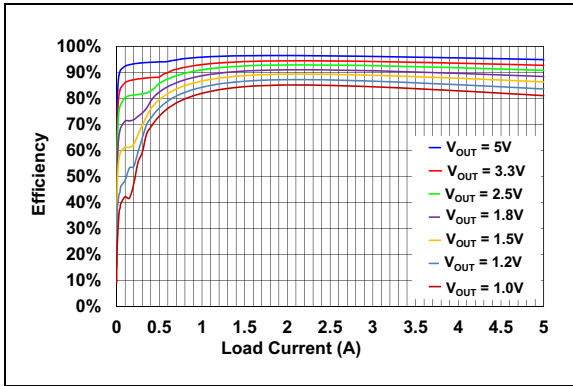


FIGURE 2-25: Efficiency vs. Output Current (Input Voltage = 12V, HLL Mode).

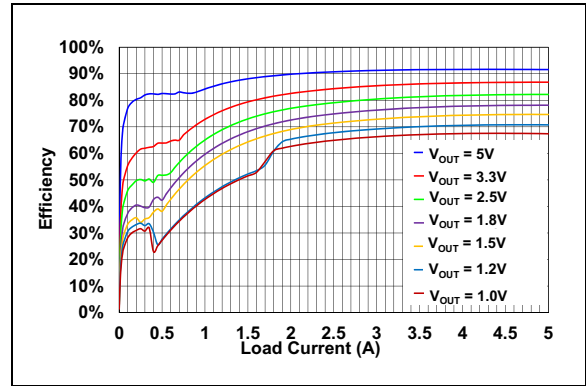


FIGURE 2-28: Efficiency vs. Output Current (Input Voltage = 48V, HLL Mode).

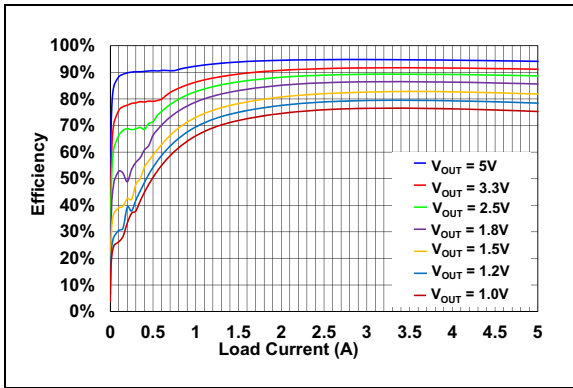


FIGURE 2-26: Efficiency vs. Output Current (Input Voltage = 24V, HLL Mode).

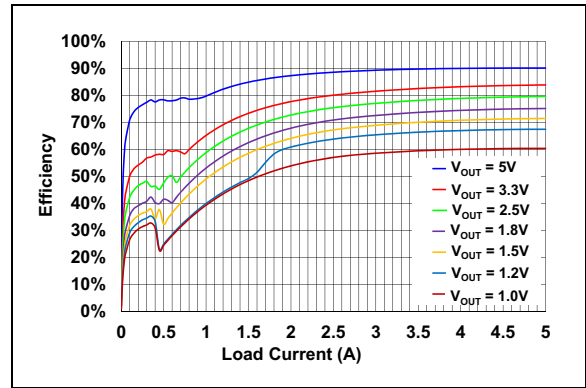


FIGURE 2-29: Efficiency vs. Output Current (Input Voltage = 60V, HLL Mode).

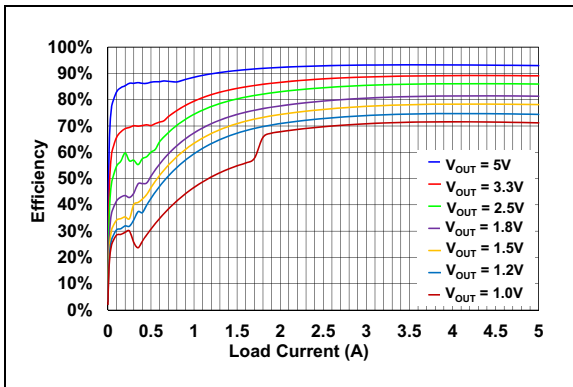


FIGURE 2-27: Efficiency vs. Output Current (Input Voltage = 36V, HLL Mode).

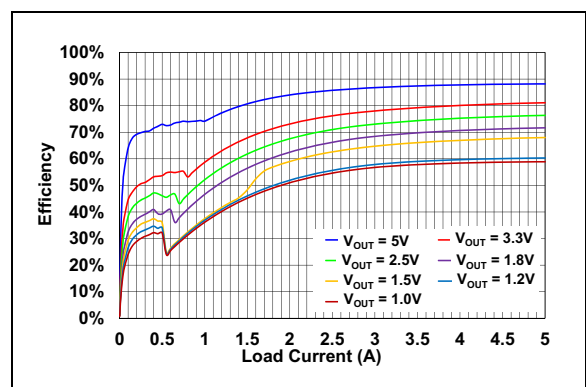


FIGURE 2-30: Efficiency vs. Output Current (Input Voltage = 75V, HLL Mode).

Note: Unless otherwise indicated, $V_{VIN} = 12V$, $f_{SW} = 300\text{ kHz}$, $R_{CL} = 1.3\text{ k}\Omega$, $L = 10\text{ }\mu\text{H}$, $V_{EXTVDD} = V_{OUT}$, $T_A = +25^\circ\text{C}$ (refer to the [Typical Application Circuit](#) circuit).

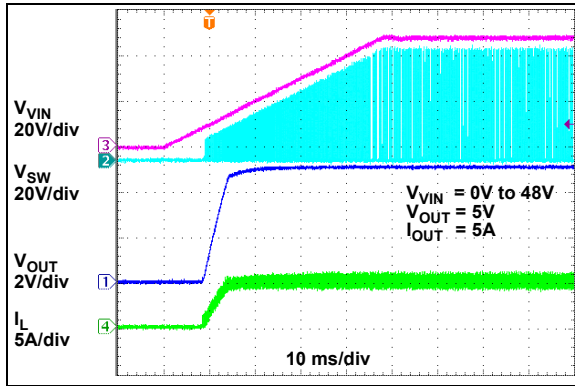


FIGURE 2-31: Power-Up.

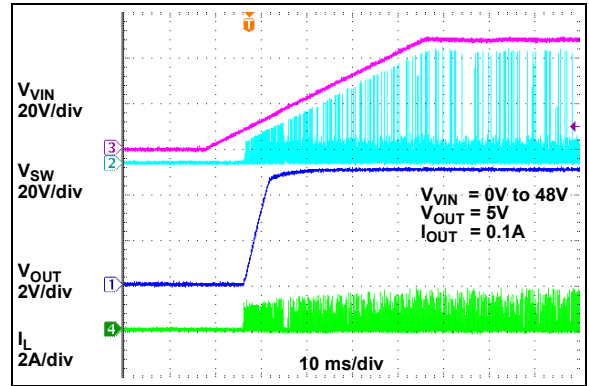


FIGURE 2-34: Power-Up at Light Load in HLL Mode ($I_{OUT} = 0.1A$).

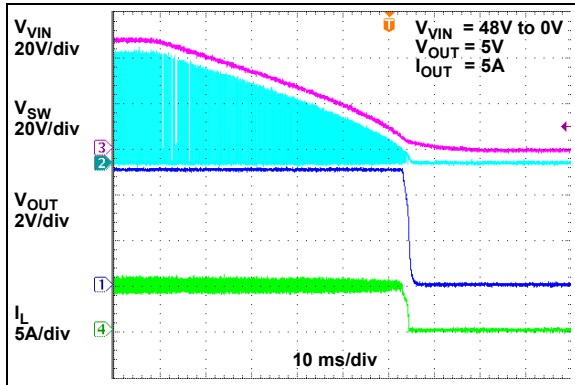


FIGURE 2-32: Power-Down.

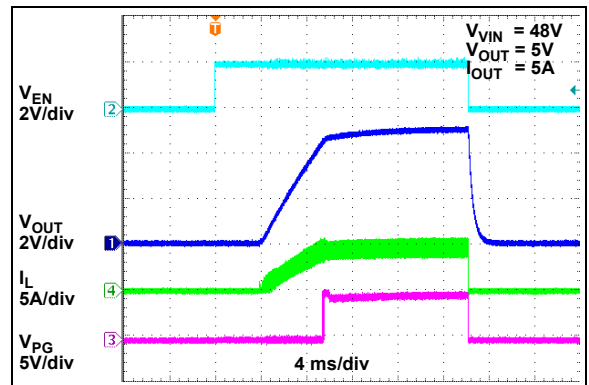


FIGURE 2-35: Enable Turn-On/Turn-Off.

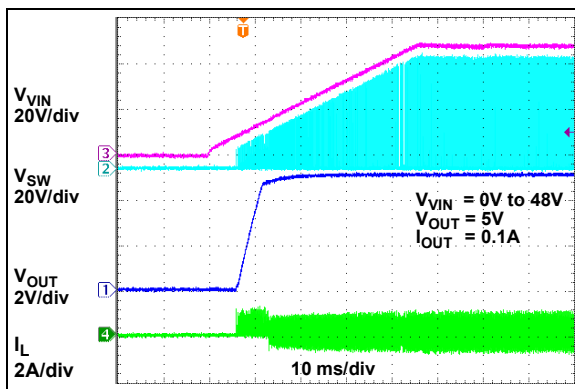


FIGURE 2-33: Power-Up at Light Load in CCM Mode ($I_{OUT} = 0.1A$).

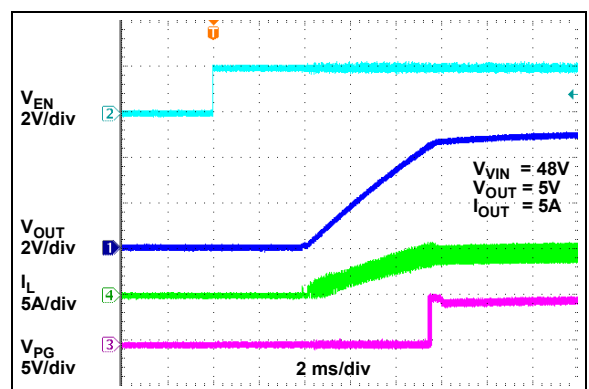


FIGURE 2-36: Enable Turn-On Delay.

Note: Unless otherwise indicated, $V_{VIN} = 12V$, $f_{SW} = 300\text{ kHz}$, $R_{CL} = 1.3\text{ k}\Omega$, $L = 10\text{ }\mu\text{H}$, $V_{EXTVDD} = V_{OUT}$, $T_A = +25^\circ\text{C}$ (refer to the [Typical Application Circuit](#) circuit).

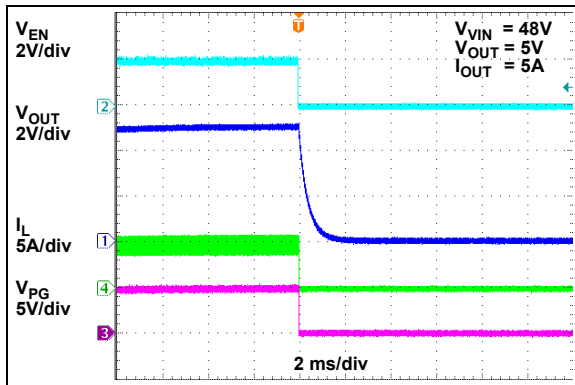


FIGURE 2-37: Enable Turn-Off Delay.

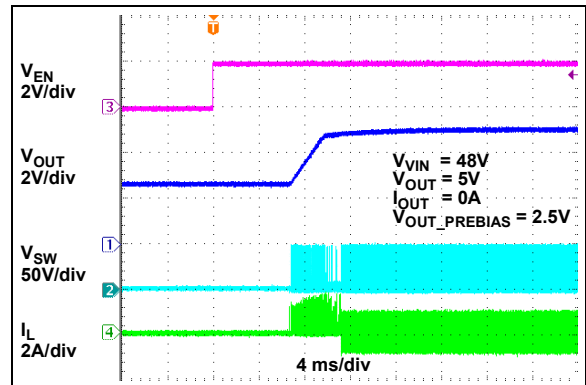


FIGURE 2-40: Enable Turn-On with Prebiased Output (CCM Mode).

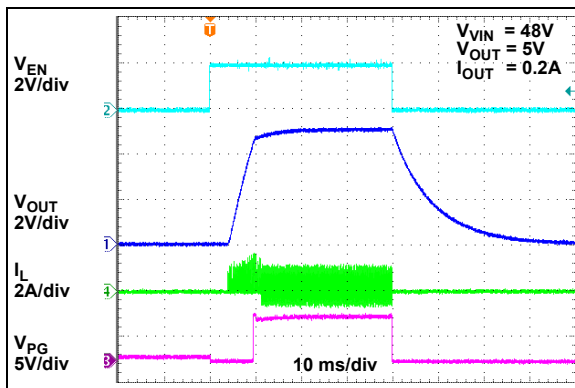


FIGURE 2-38: Enable Turn-On/Turn-Off at Light Load in CCM Mode.

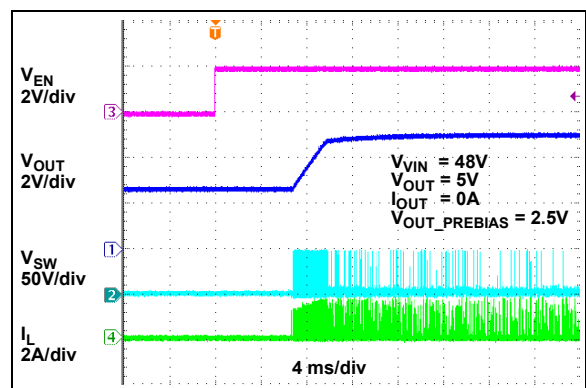


FIGURE 2-41: Enable Turn-On with Prebiased Output (HLL Mode).

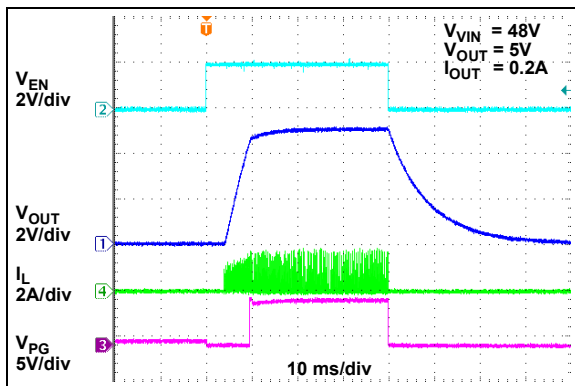


FIGURE 2-39: Enable Turn-On/Turn-Off at Light Load in HLL Mode.

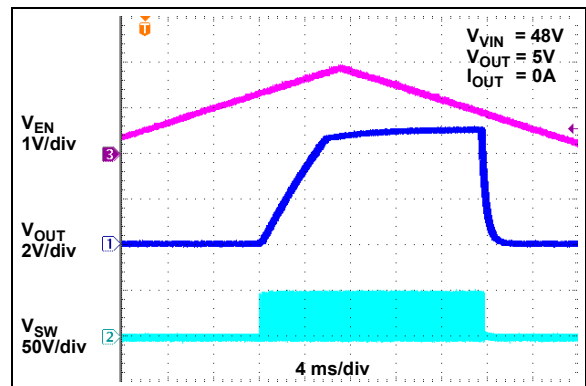


FIGURE 2-42: Enable Thresholds.

Note: Unless otherwise indicated, $V_{VIN} = 12V$, $f_{SW} = 300\text{ kHz}$, $R_{CL} = 1.3\text{ k}\Omega$, $L = 10\text{ }\mu\text{H}$, $V_{EXTVDD} = V_{OUT}$, $T_A = +25^\circ\text{C}$ (refer to the [Typical Application Circuit](#) circuit).

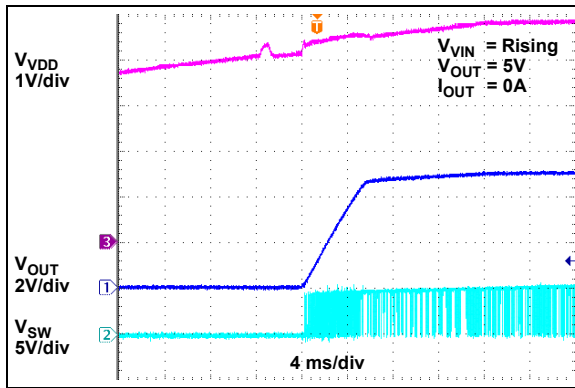


FIGURE 2-43: V_{DD} UVLO Threshold-Rising.

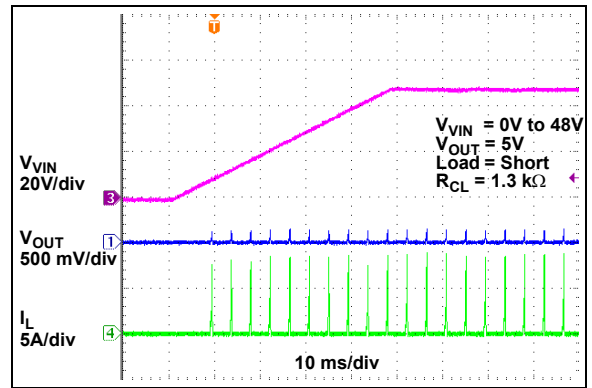


FIGURE 2-46: Power-Up into Output Short.

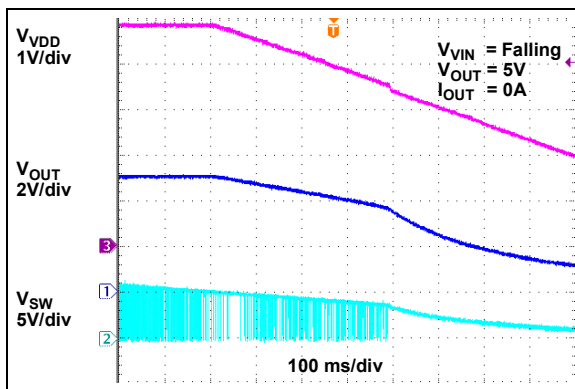


FIGURE 2-44: V_{DD} UVLO Threshold-Falling.

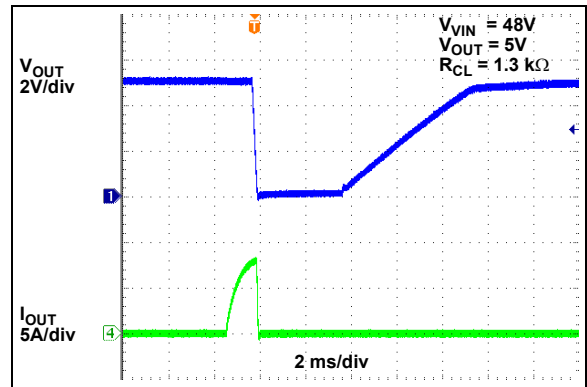


FIGURE 2-47: Output Current Limit Threshold.

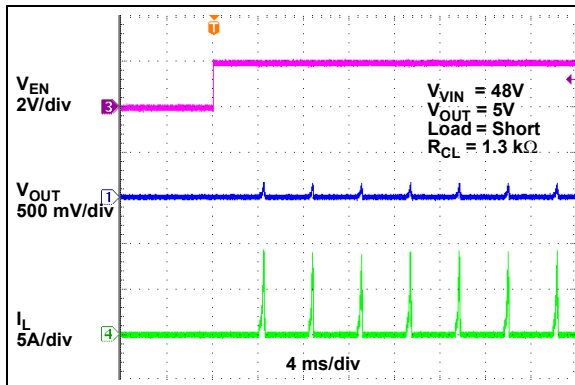


FIGURE 2-45: Enable into Output Short.

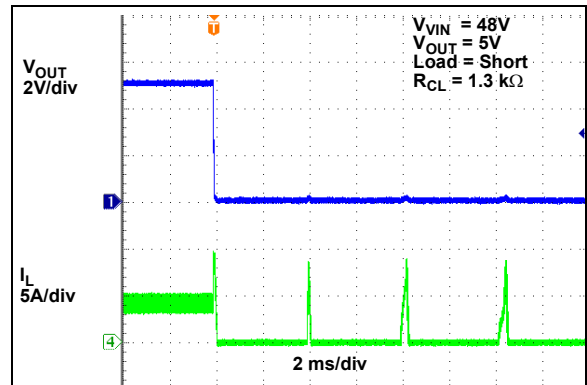


FIGURE 2-48: Output Short Circuit.

Note: Unless otherwise indicated, $V_{VIN} = 12V$, $f_{SW} = 300\text{ kHz}$, $R_{CL} = 1.3\text{ k}\Omega$, $L = 10\text{ }\mu\text{H}$, $V_{EXTVDD} = V_{OUT}$, $T_A = +25^\circ\text{C}$ (refer to the [Typical Application Circuit](#) circuit).

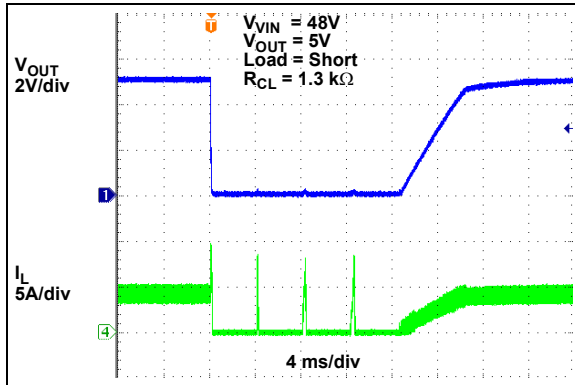


FIGURE 2-49: Recovery from Output Short Circuit.

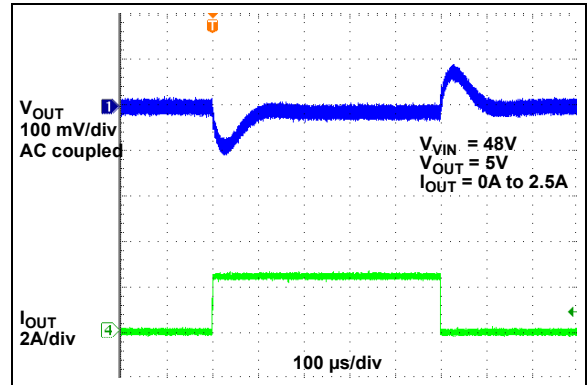


FIGURE 2-52: Load Transient Response (CCM Mode).

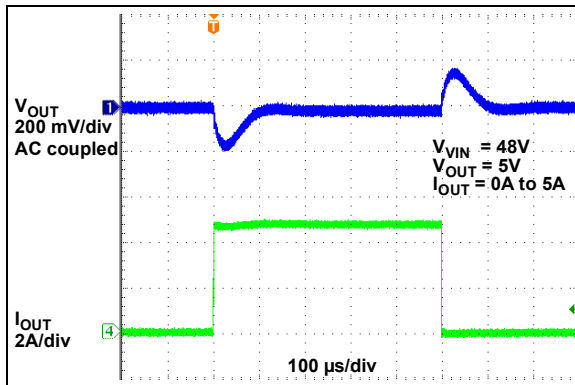


FIGURE 2-50: Load Transient Response (CCM Mode).

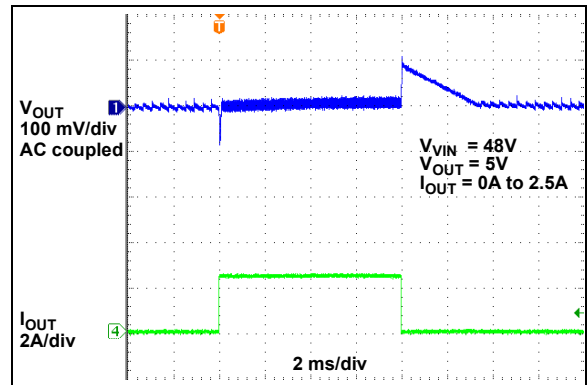


FIGURE 2-53: Load Transient Response (HLL Mode).

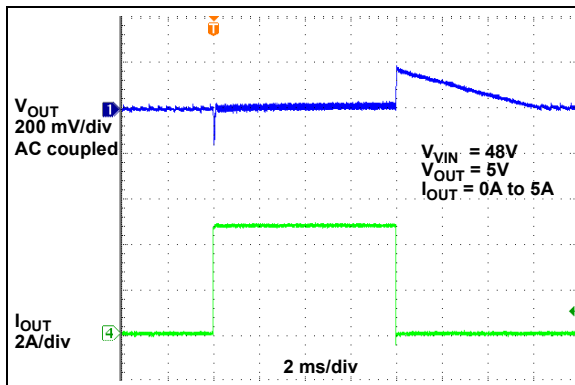


FIGURE 2-51: Load Transient Response (HLL Mode).

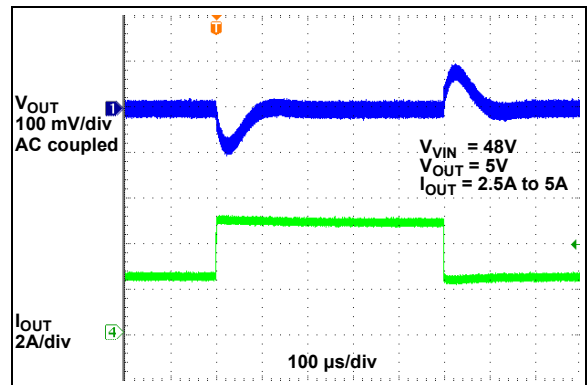


FIGURE 2-54: Load Transient Response (HLL Mode).

Note: Unless otherwise indicated, $V_{VIN} = 12V$, $f_{SW} = 300\text{ kHz}$, $R_{CL} = 1.3\text{ k}\Omega$, $L = 10\text{ }\mu\text{H}$, $V_{EXTVDD} = V_{OUT}$, $T_A = +25^\circ\text{C}$ (refer to the [Typical Application Circuit](#) circuit).

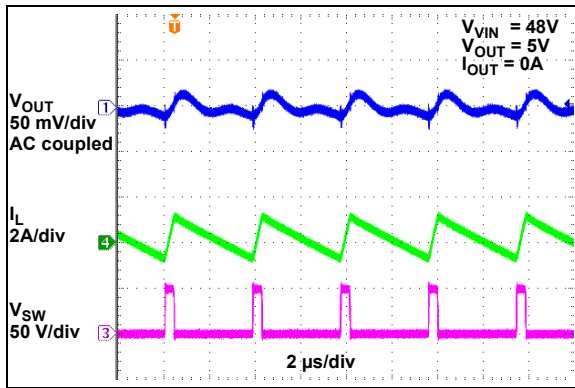


FIGURE 2-55: Switching Waveform at No Load (CCM Mode).

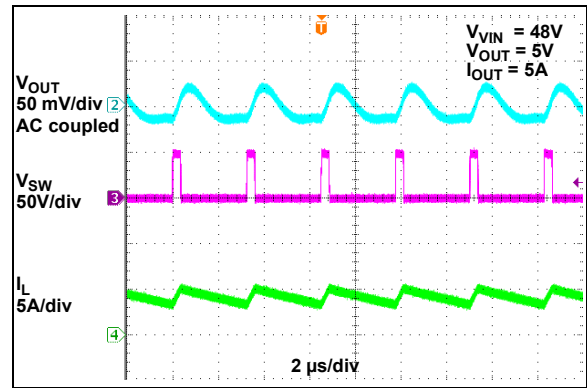


FIGURE 2-57: Switching Waveform at Full Load.

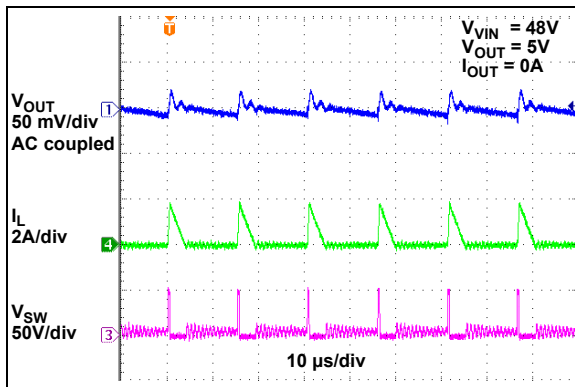


FIGURE 2-56: Switching Waveform at No Load (HLL Mode).

3.0 PIN DESCRIPTION

The descriptions of the pins are listed in [Table 3-1](#).

TABLE 3-1: PIN FUNCTION TABLE

Pin Number	Pin Name	Pin Function
1	PG	Open-drain Power Good Output Pin
2	I _{LIM}	Current Limit Setting Resistor Connection Pin
3	SW	Switch Pin and Current Sense Input for negative current limit
4	BST	Bootstrap Capacitor Connection Pin
5	DH	High-side N-MOSFET Gate Driver Output
6	P _{GND}	Power Ground
7	DL	Low-side N-MOSFET Gate Driver Output
8	P _{VDD}	Internal Low Dropout Regulators Output of the MIC2127A
9	EXTVDD	Supply Input for the internal low voltage LDO
10	EN	Enable Input
11	FREQ	Switching Frequency Programming Input
12	MODE	Light Load Mode Selection Input
13	FB	Feedback Input
14	A _{GND}	Analog Ground
15	V _{DD}	Supply Input for the MIC2127A internal analog circuits
16	V _{IN}	Supply Input for the internal high-voltage LDO
17	EP	Exposed Pad

3.1 Power Good Output Pin (PG)

Connect PG to V_{DD} through a pull-up resistor. PG is low when the FB voltage is 10% below the 0.6V reference voltage.

3.2 Current Limit Pin (I_{LIM})

Connect a resistor from I_{LIM} to SW to set the current limit. Refer to [Section 4.3 “Current Limit \(I_{LIM}\)”](#) for more details.

3.3 Switch Pin (SW)

The SW pin provides the return path for the high-side N-MOSFET gate driver when High-Side MOSFET Gate Drive (DH) is low and is also used to sense low-side MOSFET current by monitoring the SW node voltage for negative current limit function.

Connect SW to the pin where the high-side MOSFET source and the low-side MOSFET drain terminal are connected together.

3.4 Bootstrap Capacitor Pin (BST)

BST capacitor acts as supply for the high-side N-MOSFET driver. Connect a minimum of 0.1 μF low ESR ceramic capacitor between BST and SW. Refer to [Section 4.5 “High-Side MOSFET Gate Drive \(DH\)”](#) for more details.

3.5 High-Side N-MOSFET Gate Driver Output Pin (DH)

High-side N-MOSFET gate driver Output. Connect DH to the gate of external high-side N-MOSFET.

3.6 Power Ground Pin (P_{GND})

P_{GND} provides the return path for the internal low-side N-MOSFET gate driver output and also acts as reference for the current limit comparator. Connect P_{GND} to the external low-side N-MOSFET source terminal and to the return terminal of P_{VDD} bypass capacitor.

3.7 Low-Side N-MOSFET Gate Driver Output Pin (DL)

Low-side N-MOSFET gate driver output. Connect to the gate terminal of the external low-side N-MOSFET.

3.8 Internal Low Dropout Regulators Output Pin (P_{VDD})

Combined output of the two internal LDOs (one LDO powered by V_{IN} and the other LDO powered by EXTVDD). P_{VDD} is the supply for the low-side MOSFET driver and for the floating high-side MOSFET driver. Connect a minimum of 4.7 μF low ESR ceramic capacitor from P_{VDD} to P_{GND}.

3.9 EXTVD

Supply to the internal low voltage LDO. Connect EXTVD to the output of the buck converter if it is between 4.7V to 14V to improve system efficiency. Bypass EXTVD with a minimum of 1 μ F low ESR ceramic capacitor. Refer to [Section 4.7 “Auxiliary Bootstrap LDO \(EXTVD\)”](#) for more details.

3.10 Enable Input Pin (EN)

EN is a logic input. Connect to logic high to enable the converter, and connect to logic low to disable the converter.

3.11 Switching Frequency Programming Input Pin (FREQ)

Switching Frequency Programming Input. Connect to mid-point of the resistor divider formed between V_{IN} and A_{GND} to set the switching frequency of the converter. Tie FREQ to V_{IN} to set the switching frequency to 800 kHz. Refer to [Section 5.1 “Setting the Switching Frequency”](#) for more details.

3.12 Light Load Mode Selection Input Pin (MODE)

Light Load Mode Selection Input. Connect MODE pin to V_{DD} to select Continuous Conduction mode under light loads, or connect to A_{GND} to select HyperLight Load (HLL) mode of operation under light loads. Refer to [Section 4.2 “Light Load Operating Mode \(MODE\)”](#) for further details.

3.13 Feedback Input Pin (FB)

FB is input to the transconductance amplifier of the control loop. The control loop regulates the FB voltage to 0.6V. Connect the FB node to the mid-point of the resistor divider between output and A_{GND} .

3.14 Analog Ground Pin (A_{GND})

A_{GND} is the reference to the analog control circuits inside the MIC2127A. Connect A_{GND} to P_{GND} at one point on the PCB.

3.15 Bias Voltage Pin (V_{DD})

Supply for the MIC2127A internal analog circuits. Connect V_{DD} to P_{VDD} of the MIC2127A through a low-pass filter. Connect a minimum of 4.7 μ F low ESR ceramic capacitor from V_{DD} to A_{GND} for decoupling.

3.16 Input Voltage Pin (V_{IN})

Supply Input to the internal high-voltage LDO. Connect to the main power source and bypass to P_{GND} with a minimum of 0.1 μ F low ESR ceramic capacitor.

3.17 Exposed Pad (EP)

Connect to the A_{GND} copper plane to improve thermal performance of the MIC2127A device.

4.0 FUNCTIONAL DESCRIPTION

The MIC2127A device is an adaptive on-time synchronous buck controller, designed to cover a wide range of input voltage applications ranging from 4.5V-5V. An adaptive on-time control scheme is employed to get a fast transient response and to obtain high-voltage conversion ratios at constant switching frequency. Overcurrent protection is implemented by sensing low-side MOSFET's $R_{DS(ON)}$, which eliminates lossy current sense resistor. The device features internal soft-start, enable input, UVLO, power good output (PG), secondary bootstrap LDO and thermal shutdown.

4.1 Theory of Operation

The MIC2127A is an adaptive on-time synchronous buck controller that operates based on ripple at the feedback node. The output voltage is sensed by the MIC2127A feedback pin (FB) and is compared to a 0.6V reference voltage (V_{REF}) at the low-gain transconductance error amplifier (g_M), as shown in the [Functional Block Diagram](#). [Figure 4-1](#) shows the MIC2127A control loop timing during steady-state operation.

The error amplifier behaves as the short circuit for the ripple voltage frequency on the FB pin, which causes the error amplifier output voltage ripple to follow the feedback voltage ripple. When the transconductance error amplifier output (V_{gM}) is below the reference voltage of the comparator, which is same as the error amplifier reference (V_{REF}), the comparator triggers and generates an on-time event. The on-time period is predetermined by the fixed t_{ON} estimator circuitry, which is given by [Equation 4-1](#):

EQUATION 4-1:

$$t_{ON(ESTIMATED)} = \frac{V_{OUT}}{V_{VIN} \times f_{SW}}$$

Where:

V_{OUT} = Output voltage
 V_{VIN} = Power stage input voltage
 f_{SW} = Switching frequency

At the end of the ON time, the internal high-side driver turns off the high-side MOSFET and the low-side driver turns on the low-side MOSFET. The OFF time of the high-side MOSFET depends on the feedback voltage. When the feedback voltage decreases, the output of the g_M amplifier (V_{gM}) also decreases. When the output of the g_M amplifier (V_{gM}) is below the reference voltage of the comparator (which is same as the error amplifier reference (V_{REF})), the OFF time ends and ON time is triggered. If the OFF time determined by the feedback voltage is less than the minimum OFF time ($t_{OFF(MIN)}$) of the MIC2127A, which is about 230 ns (typical), the MIC2127A control logic applies the $t_{OFF(MIN)}$, instead.

The maximum duty cycle can be calculated using [Equation 4-2](#):

EQUATION 4-2:

$$D_{MAX} = \frac{t_{SW} - t_{OFF(MIN)}}{t_{SW}} = 1 - \frac{230 \text{ ns}}{t_{SW}}$$

Where:

t_{SW} = Switching period, equal to $1/f_{SW}$

It is not recommended to use the MIC2127A device with an OFF time close to $t_{OFF(MIN)}$ during steady-state operation.

The adaptive on-time control scheme results in a constant switching frequency over the wide range of input voltage and load current. The actual ON time and resulting switching frequency varies with the different rising and falling times of the external MOSFETs. The minimum controllable ON time ($t_{ON(MIN)}$) results in a lower switching frequency than the target switching frequency in high V_{IN} to V_{OUT} ratio applications.

[Equation 4-3](#) shows the output-to-input voltage ratio, below which the MIC2127A device lowers the switching frequency in order to regulate the output to set value.

EQUATION 4-3:

$$\frac{V_{OUT}}{V_{IN}} \geq t_{ON(MIN)} \times f_{SW}$$

Where:

V_{OUT} = Output voltage
 V_{IN} = Input voltage
 f_{SW} = Switching frequency
 $t_{ON(MIN)}$ = Minimum controllable ON time (80 ns typ.)

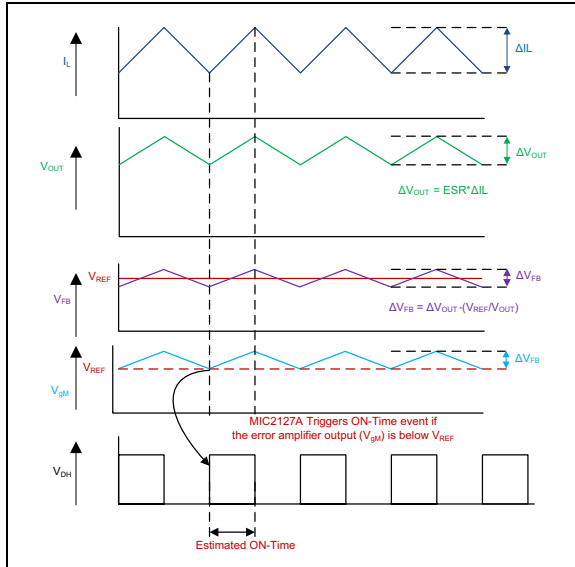


FIGURE 4-1: MIC2127A Control Loop Timing.

Figure 4-2 shows operation of the MIC2127A during load transient. The output voltage drops due to a sudden increase in load, which results in the error amplifier output (V_{gM}) falling below V_{REF} . This causes the comparator to trigger an on-time event. At the end of the ON time, a minimum OFF time $t_{OFF(MIN)}$ is generated to charge the bootstrap capacitor. The next ON time is triggered immediately after the $t_{OFF(MIN)}$ if the error amplifier output voltage (V_{gM}) is still below V_{REF} due to the low feedback voltage. This operation results in higher switching frequency during load transients. The switching frequency returns to the nominal set frequency once the output stabilizes at new load current level. The output recovery time is fast and the output voltage deviation is small in the MIC2127A converter due to the varying duty cycle and switching frequency.

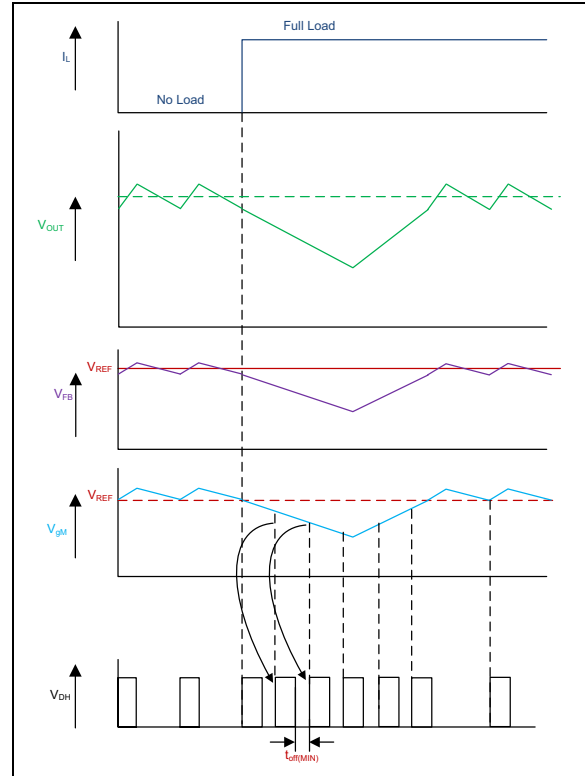


FIGURE 4-2: MIC2127A Load Transient Response.

Unlike true current-mode control, the MIC2127A uses the output voltage ripple to trigger an on-time event. In order to meet the stability requirements, the MIC2127A feedback voltage ripple should be in phase with the inductor current ripple and large enough to be sensed by the internal error amplifier. The recommended feedback voltage ripple is approximately 20 mV-100 mV over the full input voltage range. If a low-ESR output capacitor is selected, then the feedback voltage ripple may be too small to be sensed by the internal error amplifier. Also, the output voltage ripple and the feedback voltage ripple are not necessarily in phase with the inductor current ripple if the ESR of the output capacitor is very low. For these applications, ripple injection is required to ensure proper operation. Refer to [Section 5.7 “Ripple Injection”](#) for details about the ripple injection technique.

4.2 Light Load Operating Mode (MODE)

MIC2127A features a MODE pin that allows the user to select either Continuous Conduction mode or HyperLight Load (HLL) mode under light loads. HLL mode increases the system efficiency at light loads by reducing the switching frequency. Continuous Conduction mode keeps the switching frequency almost constant over the load current range.

Figure 4-3 shows the control loop timing in HLL mode. The MIC2127A device has a zero crossing comparator (ZC Detection) that monitors the inductor current by sensing the voltage drop across the low-side MOSFET during its ON time. The zero crossing comparator triggers whenever the low-side MOSFET current goes negative and turns off the low-side MOSFET. The switching instant of the high-side MOSFET depends on the error amplifier output, which is same as the comparator inverting input (see the [Functional Block Diagram](#)). If the error amplifier output is higher than the comparator reference, then the MIC2127A enters into Sleep mode. During Sleep mode, both the high-side and low-side MOSFETs are kept off and the efficiency is optimized by shutting down all the nonessential circuits inside the MIC2127A. The load current is supplied by the output capacitor during Sleep mode. The control circuitry wakes up when the error amplifier output falls below the comparator reference and a t_{ON} pulse is triggered.

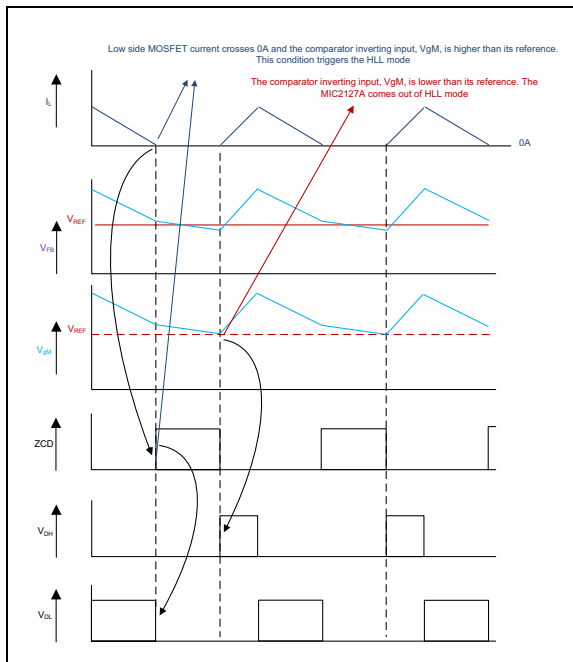


FIGURE 4-3: MIC2127A Control Loop Timing (HLL Mode).

The typical no-load supply current during HLL mode is only about 300 μ A, allowing the MIC2127A device to achieve high efficiency at light load operation.

4.3 Current Limit (I_{LIM})

The MIC2127A device uses the low-side MOSFET $R_{DS(ON)}$ to sense inductor current. In each switching cycle of the MIC2127A converter, the inductor current is sensed by monitoring the voltage across the low-side MOSFET during the OFF period of the switching cycle, during which low-side MOSFET is ON. An internal current source of 100 μ A generates a voltage across the external current limit setting resistor R_{CL} as shown in Figure 4-4.

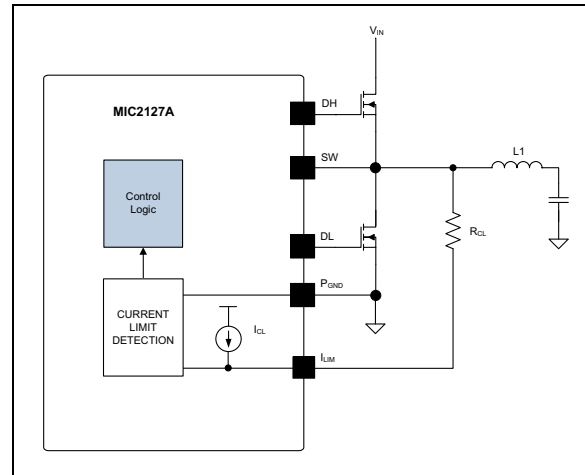


FIGURE 4-4: MIC2127A Current Limiting Circuit.

The I_{LIM} pin voltage (V_{LIM}) is the difference of the voltage across the low-side MOSFET and the voltage across the resistor (V_{RCL}). The sensed voltage V_{LIM} is compared with the power ground (P_{GND}) after a blanking time of 150 ns.

If the absolute value of the voltage drop across the low-side MOSFET is greater than the absolute value of the voltage across the current setting resistor (V_{RCL}), the MIC2127A triggers the current limit event. Consecutive eight-current limit events trigger the hiccup mode. Once the controller enters into hiccup mode, it initiates a soft start sequence after a hiccup timeout of 4 ms (typical). Both the high-side and low-side MOSFETs are turned off during hiccup timeout. The hiccup sequence, including the soft start, reduces the stress on the switching FETs and protects the load and supply from severe short conditions.

The current limit can be programmed by using the following [Equation 4-4](#).

EQUATION 4-4:

$$R_{CL} = \frac{\left(I_{CLIM} + \frac{\Delta I_{LPP}}{2}\right) \times R_{DS(ON)} + V_{OFFSET}}{I_{CL}}$$

Where:

I_{CLIM}	= Load current limit
$R_{DS(ON)}$	= On-resistance of low-side power MOSFET
ΔI_{LPP}	= Inductor peak-to-peak ripple current
V_{OFFSET}	= Current-limit comparator offset (15 mV max.)
I_{CL}	= Current-limit source current (100 μ A typ)

Since MOSFET $R_{DS(ON)}$ varies from 30%-40% with temperature, it is recommended to consider the $R_{DS(ON)}$ variation while calculating R_{CL} in the above equation, to avoid false current limiting due to increased MOSFET junction temperature rise. Also connect the SW pin directly to the drain of the low-side MOSFET to accurately sense the MOSFET's $R_{DS(ON)}$.

To improve the current limit variation, the MIC2127A adjusts the internal source current of the current limit (I_{CL}) at a rate of 0.3 μ A/ $^{\circ}$ C when the MIC2127A junction temperature changes to compensate the $R_{DS(ON)}$ variation of external low-side MOSFET. The effectiveness of this method depends on the thermal gradient between the MIC2127A and the external low-side MOSFET. The lower the thermal gradient, the better the current limit variation.

A small capacitor (C_{CL}) can be connected from the I_{LIM} pin to P_{GND} to filter the switch node ringing during the OFF time, allowing a better current sensing. The time constant of R_{CL} and C_{CL} should be less than the minimum OFF time.

4.4 Negative Current Limit

The MIC2127A device implements negative current limit by sensing the SW voltage when the low-side FET is ON. If the SW node voltage exceeds 48 mV typical, the device turns off the low-side FET for 500 ns. Negative current limit value is shown in [Equation 4-5](#).

EQUATION 4-5:

$$I_{NLIM} = \frac{48mV}{R_{DS(ON)}}$$

Where:

I_{NLIM}	= Negative current limit
$R_{DS(ON)}$	= On-resistance of low-side power MOSFET

4.5 High-Side MOSFET Gate Drive (DH)

The MIC2127A's high-side drive circuit is designed to switch an N-Channel external MOSFET. The MIC2127A [Functional Block Diagram](#) shows a

bootstrap diode between the P_{VDD} and BST pins. This circuit supplies energy to the high-side drive circuit. A low ESR ceramic capacitor should be connected between BST and SW pins (refer to the [Typical Application Circuit](#) circuit). The capacitor between BST and SW pins, C_{BST} , is charged while the low-side MOSFET is on. When the high-side MOSFET driver is turned on, energy from C_{BST} is used to turn the MOSFET on. A minimum of 0.1 μ F low ESR ceramic capacitor is recommended between BST and SW pins. The required value of C_{BST} can be calculated using the following [Equation 4-6](#):

EQUATION 4-6:

$$C_{BST} = \frac{Q_{G_HS}}{\Delta V_{CBST}}$$

Where:

Q_{G_HS}	= High-side MOSFET total gate charge
ΔV_{CBST}	= Voltage drop across the C_{BST} , generally 50 mV to 100 mV

A small resistor in series with C_{BST} can be used to slow down the turn-on time of the high-side N-channel MOSFET.

4.6 Low-Side MOSFET Gate Drive (DL)

MIC2127A's low-side drive circuit is designed to switch an N-Channel external MOSFET. The internal low-side MOSFET driver is powered by P_{VDD} . Connect a minimum of 4.7 μ F low-ESR ceramic capacitor to supply the transient gate current of the external MOSFET.

4.7 Auxiliary Bootstrap LDO (EXTVDD)

MIC2127A features an auxiliary bootstrap LDO that improves the system efficiency by supplying the MIC2127A internal circuit bias power and gate drivers from the converter output voltage. This LDO is enabled when the voltage on the EXTVDD pin is above 4.6V (typical) and, at the same time, the main LDO that operates from V_{IN} is disabled to reduce power consumption. Connect EXTVDD to the output of the buck converter if it is between 4.7V and 14V. When the EXTVDD is tied to V_{OUT} , a voltage spike will occur at the P_{VDD} and V_{DD} during a fast hard short at V_{OUT} . Larger decoupling ceramic capacitors of 10 μ F at P_{VDD} and V_{DD} are recommended for such a situation.

5.0 APPLICATIONS INFORMATION

5.1 Setting the Switching Frequency

The MIC2127A device is an adjustable-frequency, synchronous buck controller, featuring a unique adaptive on-time control architecture. The switching frequency can be adjusted between 270 kHz-800 kHz by changing the resistor divider network between V_{IN} and A_{GND} pins consisting of R_1 and R_2 , as shown in Figure 5-1.

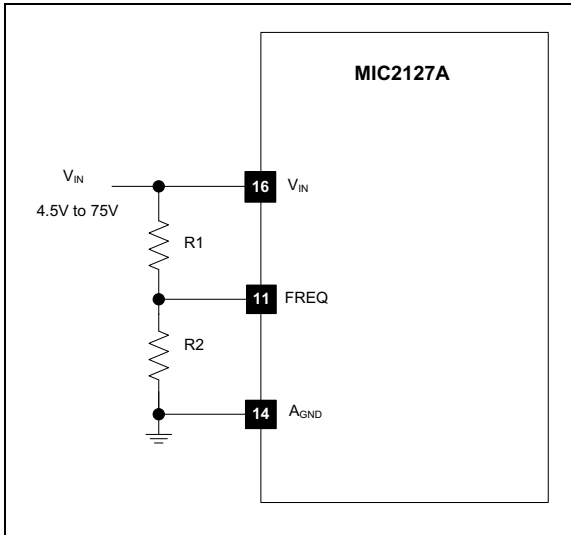


FIGURE 5-1: Switching Frequency Adjustment.

Equation 5-1 shows the estimated switching frequency.

EQUATION 5-1:

$$f_{SW_ADJ} = f_O \times \frac{R_2}{R_1 + R_2}$$

f_O is the switching frequency when R_1 is 100 k Ω and R_2 being open; f_O is typically 800 kHz. For more precise setting, it is recommended to use Figure 5-2.

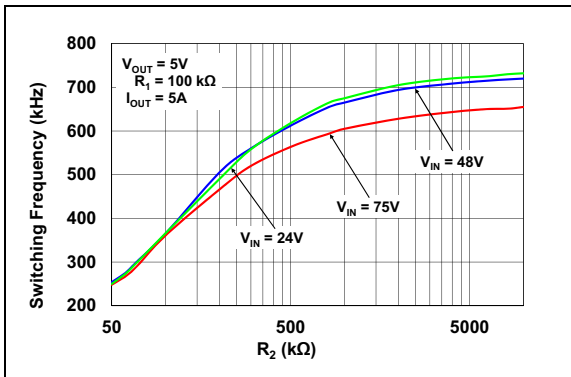


FIGURE 5-2: Switching Frequency vs. R_2 .

5.2 Output Voltage Setting

The output voltage can be adjusted using a resistor divider from output to A_{GND} whose mid-point is connected to the FB pin, as shown the Figure 5-3.

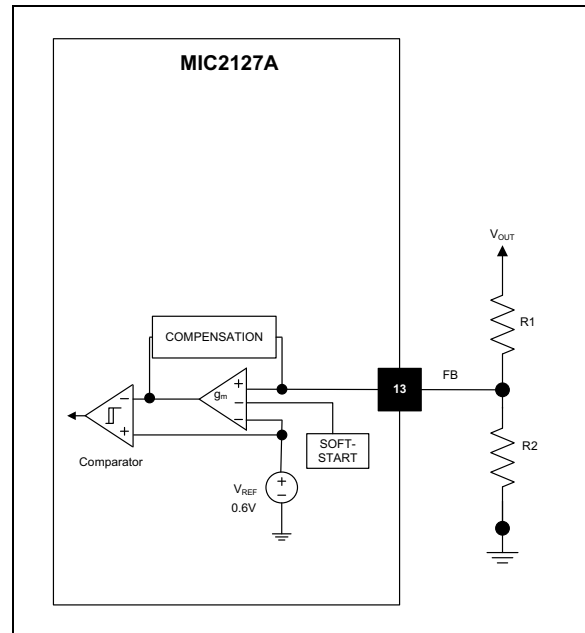


FIGURE 5-3: Output Voltage Adjustment.

The output voltage can be calculated using Equation 5-2.

EQUATION 5-2:

$$V_{OUT} = V_{REF} \times \left(1 + \frac{R_1}{R_2} \right)$$

Where:
 $V_{REF} = 0.6V$

The maximum output voltage that can be programmed using the MIC2127A is limited to 30V, if not limited by the maximum duty cycle (see Equation 4-2).

A typical value of R_1 is less than 30 k Ω . If R_1 is too large, it may allow noise to be introduced into the voltage feedback loop. It also increases the offset between the set output voltage and actual output voltage because of the error amplifier bias current. If R_1 is too small in value, it will decrease the efficiency of the power supply, especially at light loads. Once R_1 is selected, R_2 can be calculated using Equation 5-3.

EQUATION 5-3:

$$R_2 = \frac{R_1}{\frac{V_{OUT}}{V_{REF}} - 1}$$

5.3 MOSFET Selection

Important parameters for MOSFET selection are:

- Voltage rating
- On-resistance
- Total gate charge

The voltage rating for the high-side and low-side MOSFETs is essentially equal to the power stage input voltage V_{IN} . A safety factor of 30% should be added to the $V_{IN(MAX)}$ while selecting the voltage rating of the MOSFETs to account for voltage spikes due to circuit parasitic elements.

5.3.1 HIGH-SIDE MOSFET POWER LOSSES

The total power loss in the high-side MOSFET (P_{HSFET}) is the sum of the power losses because of conduction ($P_{CONDUCTION}$), switching (P_{SW}), reverse recovery charge of low-side MOSFET body diode (P_{Qrr}) and MOSFET's output capacitance discharge, as calculated in the [Equation 5-4](#).

EQUATION 5-4:

$$P_{HSFET} = P_{CONDUCTION(HS)} + P_{SW(HS)} + P_{Qrr} + P_{COSS}$$

$$P_{CONDUCTION(HS)} = (I_{RMS(HS)})^2 \times R_{DS(ON_HS)}$$

$$P_{SW(HS)} = 0.5 \times V_{IN} \times I_{LOAD} \times (t_R + t_F) \times f_{SW}$$

$$P_{Qrr} = V_{IN} \times Q_{rr} \times f_{SW}$$

$$P_{COSS} = \frac{1}{2} \times (C_{OSS(HS)} + C_{OSS(LS)}) \times (V_{IN})^2 \times f_{SW}$$

Where:

- $R_{DS(ON_HS)}$ = On-resistance of the high-side MOSFET
- V_{IN} = Operating input voltage
- I_{LOAD} = Load current
- f_{SW} = Operating switching frequency
- Q_{rr} = Reverse recovery charge of low-side MOSFET body diode or of external diode across low-side MOSFET
- $C_{OSS(HS)}$ = Effective high-side MOSFET output capacitance
- $C_{OSS(LS)}$ = Effective low-side MOSFET output capacitance
- $I_{RMS(HS)}$ = RMS current of the high-side MOSFET which can be calculated using [Equation 5-5](#).
- t_R, t_F = The high-side MOSFET turn-on and turn-off transition times which can be approximated by [Equation 5-7](#) and [Equation 5-8](#)

EQUATION 5-5:

$$I_{RMS(HS)} = I_{LOAD} \times \sqrt{D}$$

I_{LOAD} is the load current and D is the operating duty cycle, given by [Equation 5-6](#).

EQUATION 5-6:

$$D = \frac{V_{OUT}}{V_{IN}}$$

EQUATION 5-7:

$$t_R = \frac{Q_{SW(HS)} \times [R_{DH(PULL_UP)} + R_{HS(GATE)}]}{V_{DD} - V_{TH}}$$

EQUATION 5-8:

$$t_F = \frac{Q_{SW(HS)} \times [R_{DH(PULL_DOWN)} + R_{HS(GATE)}]}{V_{TH}}$$

Where:

- $R_{DH(PULL_UP)}$ = High-side gate driver pull-up resistance
- $R_{DH(PULL_DOWN)}$ = High-side gate driver pull-down resistance
- $R_{HS(GATE)}$ = High-side MOSFET gate resistance
- V_{TH} = Gate to Source threshold voltage of the high-side MOSFET
- $Q_{SW(HS)}$ = Switching gate charge of the high-side MOSFET which can be approximated by [Equation 5-9](#).

EQUATION 5-9:

$$Q_{SW(HS)} = \frac{Q_{GS(HS)}}{2} + Q_{GD(HS)}$$

Where:

- $Q_{GS(HS)}$ = High-side MOSFET gate to source charge
- $Q_{GD(HS)}$ = High-side MOSFET gate to drain charge

5.3.2 LOW-SIDE MOSFET POWER LOSSES

The total power loss in the low-side MOSFET (P_{LSFET}) is the sum of the power losses because of conduction ($P_{CONDUCTION(LS)}$) and body diode conduction during the dead time (P_{DT}), as calculated in [Equation 5-10](#).

EQUATION 5-10:

$$P_{LSFET} = P_{CONDUCTION(LS)} + P_{DT}$$

$$P_{CONDUCTION(LS)} = (I_{RMS(LS)})^2 \times R_{DS(ON_LS)}$$

$$P_{DT} = 2 \times V_F \times I_{LOAD} \times t_{DT} \times f_{SW}$$

Where:

- $R_{DS(ON_LS)}$ = On-resistance of the low-side MOSFET
- V_F = Low-side MOSFET body diode forward voltage drop
- t_{DT} = Dead time which is approximately 20 ns
- f_{SW} = Switching Frequency
- $I_{RMS(LS)}$ = RMS current of the low-side MOSFET which can be calculated using [Equation 5-11](#)

EQUATION 5-11:

$$I_{RMS(LS)} = I_{LOAD} \times \sqrt{1-D}$$

Where:

- I_{LOAD} = load current
- D = operating duty cycle

5.4 Inductor Selection

Inductance value, saturation and RMS currents are required to select the output inductor. The input and output voltages and the inductance value determine the peak-to-peak inductor ripple current.

The lower the inductance value, the higher the peak-to-peak ripple current through the inductor, which increases the core losses in the inductor. Higher inductor ripple current also requires more output capacitance to smooth out the ripple current. The greater the inductance value, the lower the peak-to-peak ripple current, which results in a larger and more expensive inductor.

A good compromise between size, loss and cost is to set the inductor ripple current to be equal to 30% of the maximum output current.

The inductance value is calculated by [Equation 5-12](#).

EQUATION 5-12:

$$L = \frac{V_{OUT} \times (V_{IN} - V_{OUT})}{V_{IN} \times f_{SW} \times 0.3 \times I_{FL}}$$

Where:

- V_{IN} = Input voltage
- f_{SW} = Switching frequency
- I_{FL} = Full load current
- V_{OUT} = Output voltage

For a selected Inductor, the peak-to-peak inductor current ripple can be calculated using [Equation 5-13](#).

EQUATION 5-13:

$$\Delta I_{L_PP} = \frac{V_{OUT} \times (V_{IN} - V_{OUT})}{V_{IN} \times f_{SW} \times L}$$

The peak inductor current is equal to the load current plus one half of the peak-to-peak inductor current ripple which is shown in [Equation 5-14](#).

EQUATION 5-14:

$$I_{L_PK} = I_{LOAD} + \frac{\Delta I_{L_PP}}{2}$$

The RMS and saturation current ratings of the selected inductor should be at least equal to the RMS current and saturation current calculated in [Equation 5-15](#) and [Equation 5-16](#).

EQUATION 5-15:

$$I_{L_RMS} = \sqrt{(I_{LOAD(MAX)})^2 + \frac{(\Delta I_{L_PP})^2}{12}}$$

Where:

- $I_{LOAD(MAX)}$ = Maximum load current

EQUATION 5-16:

$$I_{L_SAT} = \frac{(R_{CL} \times I_{CL}) + 15mV}{R_{DS(ON)}}$$

Where:

- R_{CL} = Current limit resistor
- I_{CL} = Current-Limit Source Current (100 μ A typical)
- $R_{DS(ON)}$ = On-resistance of low-side power MOSFET

Maximizing efficiency requires the proper selection of core material and minimizing the winding resistance. Use of ferrite materials is recommended in the higher switching frequency applications. Lower-cost iron powder cores may be used, but the increase in core loss reduces the efficiency of the power supply. This is especially noticeable at low output power. The winding resistance decreases efficiency at the higher output current levels. The winding resistance must be minimized, although this usually comes at the expense of a larger inductor. The power dissipated in the inductor is equal to the sum of the core and copper losses. At higher output loads, the core losses are usually insignificant and can be ignored. At lower output currents, the core losses can be a significant contributor. Core loss information is usually available from the magnetic's vendor.

The amount of copper loss in the inductor is calculated by [Equation 5-17](#).

EQUATION 5-17:

$$P_{INDUCTOR(CU)} = (I_{L_RMS})^2 \times R_{DCR}$$

5.5 Output Capacitor Selection

The main parameters for selecting the output capacitor are capacitance value, voltage rating and RMS current rating. The type of the output capacitor is usually determined by its equivalent series resistance (ESR). Recommended capacitor types are ceramic, tantalum, low-ESR aluminum electrolytic, OS-CON and POSCAP. The output capacitor ESR also affects the control loop from a stability point of view. The maximum value of ESR can be calculated using [Equation 5-18](#).

EQUATION 5-18:

$$ESR \leq \frac{\Delta V_{OUT_PP}}{\Delta I_{L_PP}}$$

Where:

ΔV_{OUT_PP} = Peak-to-peak output voltage ripple

ΔI_{L_PP} = Peak-to-peak inductor current ripple

The required output capacitance to meet steady state output voltage ripple can be calculated using [Equation 5-19](#).

EQUATION 5-19:

$$C_{OUT} = \frac{\Delta I_{L_PP}}{8 \times f_{SW} \times \Delta V_{OUT_PP}}$$

Where:

C_{OUT} = Output capacitance value

f_{SW} = Switching frequency

ΔV_{OUT_PP} = Steady state output voltage ripple

As described in [Section 4.1 "Theory of Operation"](#), the MIC2127A device requires at least 20 mV peak-to-peak ripple at the FB pin to ensure that the g_M amplifier and the comparator behave properly. Also, the output voltage ripple should be in phase with the inductor current. Therefore, the output voltage ripple caused by the output capacitor's value should be much smaller than the ripple caused by the output capacitor ESR. If low-ESR capacitors, such as ceramic capacitors, are selected as the output capacitors, a ripple injection circuit should be used to provide enough feedback-voltage ripple. Refer to the [Section 5.7 "Ripple Injection"](#) for details.

The voltage rating of the capacitor should be twice the output voltage for tantalum and 20% greater for aluminum electrolytic, ceramic or OS-CON. The output capacitor RMS current is calculated in [Equation 5-20](#).

EQUATION 5-20:

$$I_{C_OUT(RMS)} = \frac{\Delta I_{L_PP}}{\sqrt{12}}$$

The power dissipated in the output capacitor is shown in [Equation 5-21](#).

EQUATION 5-21:

$$P_{DIS(C_OUT)} = (I_{C_OUT(RMS)})^2 \times ESR_{C_OUT}$$

5.6 Input Capacitor Selection

The input capacitor reduces peak current drawn from the power supply and reduces noise and voltage ripple on the input. The input voltage ripple depends on the input capacitance and ESR. The input capacitance and ESR values can be calculated using [Equation 5-22](#).

EQUATION 5-22:

$$C_{IN} = \frac{I_{LOAD} \times D \times (1-D)}{\eta \times f_{SW} \times \Delta V_{IN_C}}$$

$$ESR_{C_IN} = \frac{\Delta V_{IN_ESR}}{I_{L_PK}}$$

Where:

I_{LOAD}	= Load Current
I_{L_PK}	= Peak Inductor Current
ΔV_{INC}	= Input ripple due to capacitance
ΔV_{INESR}	= Input ripple due to input capacitor ESR
η	= Power conversion efficiency

The input capacitor should be rated for ripple current rating and voltage rating. The RMS value of input capacitor current is determined at the maximum output current. The RMS current rating of the input capacitor should be greater than or equal to the input capacitor RMS current calculated using [Equation 5-23](#).

EQUATION 5-23:

$$I_{C_IN(RMS)} = I_{LOAD(MAX)} \times \sqrt{D \times (1-D)}$$

The power dissipated in the input capacitor is calculated using [Equation 5-24](#).

EQUATION 5-24:

$$P_{DISS(C_IN)} = (I_{C_IN(RMS)})^2 \times ESR_{C_IN}$$

5.7 Ripple Injection

The minimum recommended ripple at the FB pin for proper operation of the MIC2127A error amplifier and comparator is 20 mV. However, the output voltage ripple is generally designed as 1%-2% of the output voltage. For low output voltages, such as a 1V, the output voltage ripple is only 10 mV-20 mV, and the feedback voltage ripple is less than 20 mV. If the feedback voltage ripple is so small that the g_M amplifier and comparator cannot sense it, then the MIC2127A loses control and the output voltage is not regulated. In order to have sufficient V_{FB} ripple, the ripple injection method should be applied for low output voltage ripple applications.

The applications are divided into three situations according to the amount of the feedback voltage ripple:

1. Enough ripple at the feedback due to the large ESR of the output capacitor ([Figure 5-4](#)). The converter is stable without any additional ripple injection at the FB node. The feedback voltage ripple is given by [Equation 5-25](#).

EQUATION 5-25:

$$\Delta V_{FB(PP)} = \frac{R_2}{R_2 + R_1} \times ESR \times \Delta I_{L_PP}$$

ΔI_{L_PP} is the peak-to-peak value of the inductor current ripple.

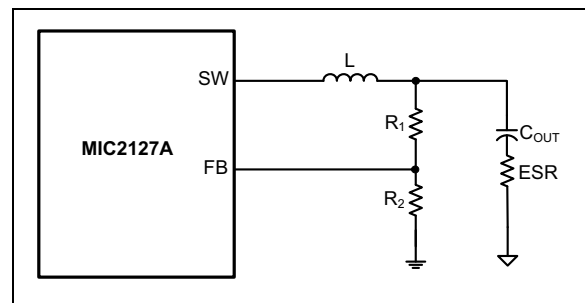


FIGURE 5-4: Enough Ripple at FB.

2. Inadequate ripple at the feedback voltage due to the small ESR of the output capacitor.

The output voltage ripple can be fed into the FB pin through a feed forward capacitor, C_{FF} in this case, as shown in [Figure 5-5](#). The typical C_{FF} value is between 1 nF-100 nF. With the feed forward capacitor, the feedback voltage ripple is very close to the output voltage ripple, which is shown in [Equation 5-26](#).

EQUATION 5-26:

$$\Delta V_{FB(PP)} = ESR \times \Delta I_{L_PP}$$

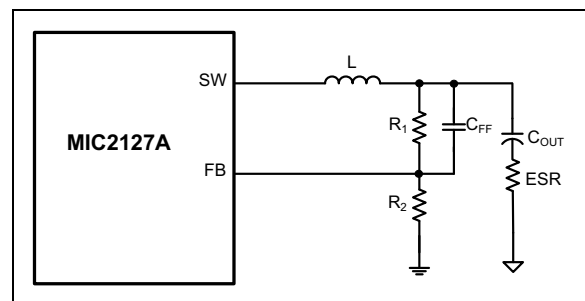


FIGURE 5-5: Inadequate Ripple at FB.

- Virtually no ripple at the FB pin voltage due to the very-low ESR of the output capacitors.

In this case, additional ripple can be injected into the FB pin from the switching node SW, via a resistor R_{INJ} and a capacitor C_{INJ} , as shown in [Figure 5-6](#).

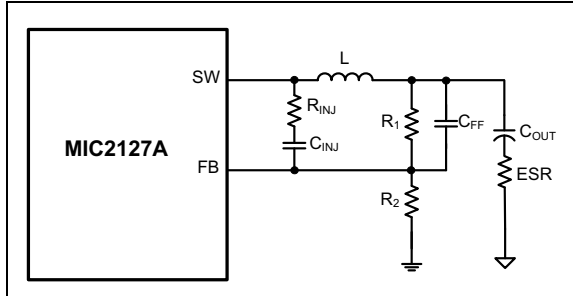


FIGURE 5-6: Invisible Ripple at FB.

The injected ripple at the FB pin in this case is given by the [Equation 5-27](#).

EQUATION 5-27:

$$\Delta V_{FB(PP)} = \frac{V_{OUT} \times (1-D)}{C_{FF} \times R_{INJ} \times f_{SW}}$$

In [Equation 5-27](#), it is assumed that the time constant associated with the C_{FF} meets the criterion shown in [Equation 5-28](#).

EQUATION 5-28:

$$\tau \geq T_{SW}$$

$$\tau = C_{FF} \times (R_1 \parallel R_2 \parallel R_{INJ})$$

The process of sizing the ripple injection resistor and capacitors is:

- Select C_{INJ} in the range of 47 nF-100 nF, which can be considered as short for a wide range of the frequencies.
- Select C_{FF} in the range of 0.47 nF-10 nF, if R_1 and R_2 are in k Ω range.
- Select R_{INJ} according to [Equation 5-29](#).

EQUATION 5-29:

$$R_{INJ} = \frac{V_{OUT} \times (1-D)}{C_{FF} \times f_{SW} \times \Delta V_{FB(PP)}}$$

Where:

- V_{OUT} = Output voltage
- D = Duty cycle
- f_{SW} = Switching frequency
- $\Delta V_{FB(PP)}$ = Injected Feedback Ripple (20 mV to 100 mV)

Once all the ripple injection component values are calculated, ensure that the criterion shown in [Equation 5-28](#) is met.

For high duty cycle applications with $D > 40\%$, the procedures to design the ripple injection circuit components are as below:

- For given feedback divider resistor values, select C_{FF} such that the time constant formed by C_{FF} and feedback divider is 50% of the switching period as given in [Equation 5-30](#):

EQUATION 5-30:

$$C_{FF} \times R_{FBEQ} = 0.5 \times T_{SW}$$

$$R_{FBEQ} = R_1 \parallel R_2 = \frac{R_1 \times R_2}{R_1 + R_2}$$

- Calculate R_{INJ} using the [Equation 5-29](#). Make sure that the injected ripple voltage into FB pin is in the range of 20 mV to 100 mV.
- Choose $C_{INJ} = 100$ nF or at least 10 times the C_{FF} value.

5.8 Power Dissipation in MIC2127A

The MIC2127A features two Low Dropout Regulators (LDOs) to supply power at the P_{VDD} pin from either V_{IN} or $EXTVDD$ depending on the voltage at the $EXTVDD$ pin. P_{VDD} powers MOSFET drivers and V_{DD} pin, which is recommended to connect to P_{VDD} through a low pass filter, powers the internal circuitry. In the applications where the output voltage is 5V and above (up to 14V), it is recommended to connect $EXTVDD$ to the output to reduce the power dissipation in the MIC2127A, to reduce the MIC2127A junction temperature and to improve the system efficiency.

The power dissipation in the MIC2127A depends on the internal LDO being in use, on the gate charge of the external MOSFETs and on the switching frequency. The power dissipation and the junction temperature of the MIC2127A can be estimated using [Equations 5-31](#), [5-32](#) and [5-33](#).

Power dissipation in the MIC2127A when $EXTVDD$ is not used.

EQUATION 5-31:

$$P_{IC} = V_{IN} \times (I_{SW} + I_Q)$$

Power dissipation in the MIC2127A when $EXTVDD$ is used.

EQUATION 5-32:

$$P_{IC} = V_{EXTVDD} \times (I_{SW} + I_Q)$$

$$I_{SW} = Q_G \times f_{SW}$$

$$Q_G = Q_{G_HS} + Q_{G_LS}$$

Where:

- I_{SW} = Switching current into the V_{IN} pin
- I_Q = Quiescent current
- Q_G = Total gate charge of the external MOSFETs which is sum of the gate charge of high-side MOSFET (Q_{G_HS}) and the low-side MOSFET (Q_{G_LS}) at 5V gate to source voltage. Gate charge information can be obtained from the MOSFETs datasheet.
- V_{EXTVDD} = Voltage at the EXTVDD pin ($4.6 \leq V_{EXTVDD} \leq 14$ V typ.)

The junction temperature of the MIC2127A can be estimated using [Equation 5-33](#).

EQUATION 5-33:

$$T_J = (P_{IC} \times \theta_{JA}) + T_A$$

Where:

- T_J = Junction temperature
- P_{IC} = Power dissipation
- θ_{JA} = Junction Ambient Thermal resistance (50.8°C/W)

The maximum recommended operating junction temperature for the MIC2127A is +125°C.

Using the output voltage of the same switching regulator, when it is between 4.6V (typ.) to 14V, as the voltage at the EXTVDD pin significantly reduces the power dissipation inside the MIC2127A. This reduces the junction temperature rise as illustrated in [Equation 5-35](#).

For the typical case of $V_{VIN} = 48V$, $V_{OUT} = 5V$, maximum ambient temperature of +85°C and 10 mA of I_{SW} , the MIC2127A junction temperature when the EXTVDD is not used is given by [Equation 5-34](#).

EQUATION 5-34:

$$P_{IC} = 48V \times (10mA + 1.5mA)$$

$$P_{IC} = 0.552W$$

$$T_J = (0.552W \times 50.8^\circ C/W) + 85^\circ C$$

$$T_J = 113^\circ C$$

When the 5V output is used as the input to the EXTVDD pin, the MIC2127A junction temperature reduces from +113°C to +88°C, as calculated in [Equation 5-35](#).

EQUATION 5-35:

$$P_{IC} = 5V \times (10mA + 1.5mA)$$

$$P_{IC} = 0.058W$$

$$T_J = (0.058W \times 50.8^\circ C/W) + 85^\circ C$$

$$T_J = 88^\circ C$$

6.0 PCB LAYOUT GUIDELINES

The PCB layout is critical to achieve reliable, stable and efficient performance. The following guidelines should be followed to ensure proper operation of the MIC2127A converter.

6.1 IC

- The ceramic bypass capacitors, which are connected to the V_{DD} and P_{VDD} pins, must be located right at the IC. Use wide traces to connect to the V_{DD} , P_{VDD} and A_{GND} , and P_{GND} pins respectively.
- The signal ground pin (A_{GND}) must be connected directly to the ground planes.
- Place the IC close to the point-of-load (POL).
- Signal and power grounds should be kept separate and connected at only one location.

6.2 Input Capacitor

- Place the input ceramic capacitors as closely as possible to the MOSFETs.
- Place several vias to the ground plane closely to the input capacitor ground terminal.

6.3 Inductor

- Keep the inductor connection to the switch node (SW) short.
- Do not route any digital lines underneath or close to the inductor.
- Keep the switch node (SW) away from the feedback (FB) pin.
- The SW pin should be connected directly to the drain of the low-side MOSFET to accurately sense the voltage across the low-side MOSFET.

6.4 Output Capacitor

- Use a copper plane to connect the output capacitor ground terminal to the input capacitor ground terminal.
- The feedback trace should be separate from the power trace and connected as closely as possible to the output capacitor. Sensing a long high-current load trace can degrade the DC load regulation.

6.5 MOSFETs

- MOSFET gate drive traces must be short and wide. The ground plane should be the connection between the MOSFET source and P_{GND} .
- Choose a low-side MOSFET with a high C_{GS}/C_{GD} ratio and a low internal gate resistance to minimize the effect of dV/dt induced turn-on.
- Use a 4.5V V_{GS} rated MOSFET. Its higher gate threshold voltage is more immune to glitches than a 2.5V or 3.3V rated MOSFET.

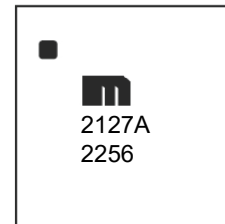
7.0 PACKAGING INFORMATION

7.1 Package Marking Information

16-Pin VQFN (3 x 3 mm)



Example

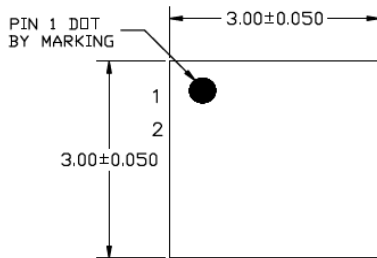


Legend:	XX...X	Product code or customer-specific information
	Y	Year code (last digit of calendar year)
	YY	Year code (last 2 digits of calendar year)
	WW	Week code (week of January 1 is week '01')
	NNN	Alphanumeric traceability code
	(e3)	Pb-free JEDEC® designator for Matte Tin (Sn)
	*	This package is Pb-free. The Pb-free JEDEC designator (e3) can be found on the outer packaging for this package.
	•, ▲, ▼	Pin one index is identified by a dot, delta up, or delta down (triangle mark).
Note:	In the event the full Microchip part number cannot be marked on one line, it will be carried over to the next line, thus limiting the number of available characters for customer-specific information. Package may or may not include the corporate logo.	
	Underbar (¯) and/or Overbar (¯) symbol may not be to scale.	

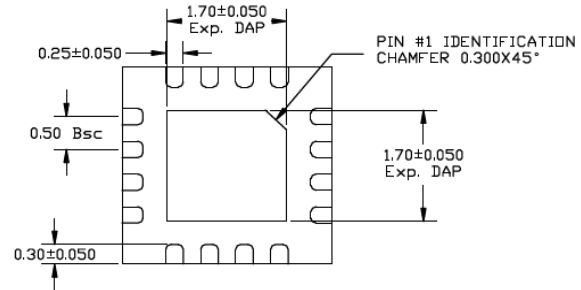
TITLE

16 LEAD QFN 3x3mm PACKAGE OUTLINE & RECOMMENDED LAND PATTERN

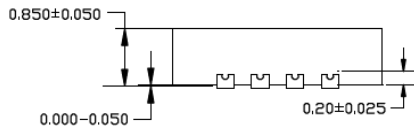
DRAWING #	QFN33-16LD-PL-3	UNIT	MM
Lead Frame	NiPdAu	Lead Finish	NiPdAu



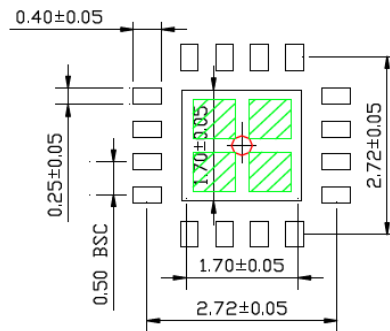
TOP VIEW
NOTE: 1, 2, 3



BOTTOM VIEW
NOTE: 1, 2, 3



SIDE VIEW
NOTE: 1, 2, 3



RECOMMENDED LAND PATTERN
NOTE: 4, 5

NOTE:

1. MAX PACKAGE WARPAGE IS 0.05mm.
2. MAX ALLOWABLE BURR IS 0.076mm IN ALL DIRECTIONS
3. PIN #1 IS ON TOP WILL BE LASER MARKED.
4. RED CIRCLE IN LAND PATTERN INDICATES THERMAL VIA. SIZE SHOULD BE 0.30-0.35mm IN DIAMETER AND SHOULD BE CONNECTED TO GND FOR MAX THERMAL PERFORMANCE.
5. GREEN RECTANGLES (SHADED AREA) INDICATE SOLDER STENCIL OPENING ON EXPOSED PAD AREA. SIZE SHOULD BE 0.60x0.60mm IN SIZE, 0.20mm SPACING.

Note: For the most current package drawings, please see the Microchip Packaging Specification located at <http://www.microchip.com/packaging>.

APPENDIX A: REVISION HISTORY

Revision F (April 2020)

The following is the list of modifications:

1. Updated content in the [Features](#) section.
2. Updated the [Typical Application Circuit](#).
3. Updated content in the [Electrical Characteristics](#) table.
4. Updated content in [Section 2.0, Typical Characteristic Curves](#).
5. Updated content in [Section 4.3, Current Limit \(ILIM\)](#).
6. Updated content in [Section 4.5, High-Side MOSFET Gate Drive \(DH\)](#).
7. Updated content in [Section 5.0, Applications Information](#).

Revision E (September 2019)

The following is the list of modifications:

1. Adds AEC-Q100 qualification for new automotive option: the MIC2127AYML-TRVAO 75V Synchronous Buck Controller.

Revision D (March 2019)

The following is the list of modifications:

2. Updated the I_{LIM} Source Current and the Zero Crossing Detection Comparator Threshold values in the [Electrical Characteristics](#) table.

Revision C (June 2018)

The following is the list of modifications:

1. Updated [Section 1.0 “Electrical Characteristics”](#).
2. Minor editorial corrections.
3. Updated Current Limit values in [Electrical Characteristics](#).
4. Updated content in [Section 3.9 “EXTVDD”](#) and [Section 4.7 “Auxiliary Bootstrap LDO \(EXTVDD\)”](#).

Revision B (December 2016)

The following is the list of modifications:

1. Minor editorial corrections.
2. Updated the Product Identification System page.

Revision A (December 2016)

- Original release of this document.

PRODUCT IDENTIFICATION SYSTEM

To order or obtain information, e.g., on pricing or delivery, refer to the factory or the listed sales office.

<u>PART NO.</u>	<u>X</u>	<u>XX</u>	<u>-XX</u>	<u>XXX</u>	
Device	Temperature	Package Code	Media Type	Qualification	
<p>Examples:</p> <p>a) MIC2127AYML-TR: 75V, Synchronous Buck Controller Featuring Adaptive On-Time Control, -40°C to +125°C junction temperature range, 16-LD VQFN package, 5000/reel</p> <p>b) MIC2127AYML-TRVAO: 75V, Synchronous Buck Controller Featuring Adaptive On-Time Control, Automotive AEC-Q100 Qualified, -40°C to +125°C junction temperature range, 16-LD VQFN package, 5000/reel</p>					
<p>Device: MIC2127A: 75V, Synchronous Buck Controller Featuring Adaptive On-Time Control</p> <p>Temperature: Y = Industrial Temperature Grade (-40°C to +125°C)</p> <p>Package: ML = 16 Lead, 3x3 mm VQFN</p> <p>Media Type: TR = 5000/reel</p> <p>Qualification: Blank = Standard Part VAO = Automotive AEC-Q100 Qualified</p>					

Note the following details of the code protection feature on Microchip devices:

- Microchip products meet the specification contained in their particular Microchip Data Sheet.
- Microchip believes that its family of products is one of the most secure families of its kind on the market today, when used in the intended manner and under normal conditions.
- There are dishonest and possibly illegal methods used to breach the code protection feature. All of these methods, to our knowledge, require using the Microchip products in a manner outside the operating specifications contained in Microchip's Data Sheets. Most likely, the person doing so is engaged in theft of intellectual property.
- Microchip is willing to work with the customer who is concerned about the integrity of their code.
- Neither Microchip nor any other semiconductor manufacturer can guarantee the security of their code. Code protection does not mean that we are guaranteeing the product as “unbreakable.”

Code protection is constantly evolving. We at Microchip are committed to continuously improving the code protection features of our products. Attempts to break Microchip's code protection feature may be a violation of the Digital Millennium Copyright Act. If such acts allow unauthorized access to your software or other copyrighted work, you may have a right to sue for relief under that Act.

Information contained in this publication regarding device applications and the like is provided only for your convenience and may be superseded by updates. It is your responsibility to ensure that your application meets with your specifications. MICROCHIP MAKES NO REPRESENTATIONS OR WARRANTIES OF ANY KIND WHETHER EXPRESS OR IMPLIED, WRITTEN OR ORAL, STATUTORY OR OTHERWISE, RELATED TO THE INFORMATION, INCLUDING BUT NOT LIMITED TO ITS CONDITION, QUALITY, PERFORMANCE, MERCHANTABILITY OR FITNESS FOR PURPOSE. Microchip disclaims all liability arising from this information and its use. Use of Microchip devices in life support and/or safety applications is entirely at the buyer's risk, and the buyer agrees to defend, indemnify and hold harmless Microchip from any and all damages, claims, suits, or expenses resulting from such use. No licenses are conveyed, implicitly or otherwise, under any Microchip intellectual property rights unless otherwise stated.

Trademarks

The Microchip name and logo, the Microchip logo, Adaptec, AnyRate, AVR, AVR logo, AVR Freaks, BesTime, BitCloud, chipKIT, chipKIT logo, CryptoMemory, CryptoRF, dsPIC, FlashFlex, flexPWR, HELDO, IGLoo, JukeBlox, KeeLoq, Klear, LANCheck, LinkMD, maXStylus, maXTouch, MediaLB, megaAVR, Microsemi, Microsemi logo, MOST, MOST logo, MPLAB, OptoLyzer, PackeTime, PIC, picoPower, PICSTART, PIC32 logo, PolarFire, Prochip Designer, QTouch, SAM-BA, SenGenuity, SpyNIC, SST, SST Logo, SuperFlash, Symmetricom, SyncServer, Tachyon, TempTrackr, TimeSource, tinyAVR, UNI/O, Vectron, and XMEGA are registered trademarks of Microchip Technology Incorporated in the U.S.A. and other countries.

APT, ClockWorks, The Embedded Control Solutions Company, EtherSynch, FlashTec, Hyper Speed Control, HyperLight Load, IntelliMOS, Libero, motorBench, mTouch, Powermite 3, Precision Edge, ProASIC, ProASIC Plus, ProASIC Plus logo, Quiet-Wire, SmartFusion, SyncWorld, Temux, TimeCesium, TimeHub, TimePictra, TimeProvider, Vite, WinPath, and ZL are registered trademarks of Microchip Technology Incorporated in the U.S.A.

Adjacent Key Suppression, AKS, Analog-for-the-Digital Age, Any Capacitor, AnyIn, AnyOut, BlueSky, BodyCom, CodeGuard, CryptoAuthentication, CryptoAutomotive, CryptoCompanion, CryptoController, dsPICDEM, dsPICDEM.net, Dynamic Average Matching, DAM, ECAN, EtherGREEN, In-Circuit Serial Programming, ICSP, INICnet, Inter-Chip Connectivity, JitterBlocker, KlearNet, KlearNet logo, memBrain, Mindi, MiWi, MPASM, MPF, MPLAB Certified logo, MPLIB, MPLINK, MultiTRAK, NetDetach, Omniscient Code Generation, PICDEM, PICDEM.net, PICKit, PICtail, PowerSmart, PureSilicon, QMatrix, REAL ICE, Ripple Blocker, SAM-ICE, Serial Quad I/O, SMART-I.S., SQI, SuperSwitcher, SuperSwitcher II, Total Endurance, TSHARC, USBCheck, VariSense, ViewSpan, WiperLock, Wireless DNA, and ZENA are trademarks of Microchip Technology Incorporated in the U.S.A. and other countries.

SQTP is a service mark of Microchip Technology Incorporated in the U.S.A.

The Adaptec logo, Frequency on Demand, Silicon Storage Technology, and Symmcom are registered trademarks of Microchip Technology Inc. in other countries.

GestIC is a registered trademark of Microchip Technology Germany II GmbH & Co. KG, a subsidiary of Microchip Technology Inc., in other countries.

All other trademarks mentioned herein are property of their respective companies.

© 2019, Microchip Technology Incorporated, All Rights Reserved.

ISBN: 978-1-5224-5885-2

For information regarding Microchip's Quality Management Systems, please visit www.microchip.com/quality.



MICROCHIP

Worldwide Sales and Service

AMERICAS

Corporate Office
2355 West Chandler Blvd.
Chandler, AZ 85224-6199
Tel: 480-792-7200
Fax: 480-792-7277
Technical Support:
<http://www.microchip.com/support>
Web Address:
www.microchip.com

Atlanta

Duluth, GA
Tel: 678-957-9614
Fax: 678-957-1455

Austin, TX

Tel: 512-257-3370

Boston

Westborough, MA
Tel: 774-760-0087
Fax: 774-760-0088

Chicago

Itasca, IL
Tel: 630-285-0071
Fax: 630-285-0075

Dallas

Addison, TX
Tel: 972-818-7423
Fax: 972-818-2924

Detroit

Novi, MI
Tel: 248-848-4000

Houston, TX

Tel: 281-894-5983

Indianapolis

Noblesville, IN
Tel: 317-773-8323
Fax: 317-773-5453
Tel: 317-536-2380

Los Angeles

Mission Viejo, CA
Tel: 949-462-9523
Fax: 949-462-9608
Tel: 951-273-7800

Raleigh, NC

Tel: 919-844-7510

New York, NY

Tel: 631-435-6000

San Jose, CA

Tel: 408-735-9110
Tel: 408-436-4270

Canada - Toronto

Tel: 905-695-1980
Fax: 905-695-2078

ASIA/PACIFIC

Australia - Sydney
Tel: 61-2-9868-6733

China - Beijing
Tel: 86-10-8569-7000

China - Chengdu
Tel: 86-28-8665-5511

China - Chongqing
Tel: 86-23-8980-9588

China - Dongguan
Tel: 86-769-8702-9880

China - Guangzhou
Tel: 86-20-8755-8029

China - Hangzhou
Tel: 86-571-8792-8115

China - Hong Kong SAR
Tel: 852-2943-5100

China - Nanjing
Tel: 86-25-8473-2460

China - Qingdao
Tel: 86-532-8502-7355

China - Shanghai
Tel: 86-21-3326-8000

China - Shenyang
Tel: 86-24-2334-2829

China - Shenzhen
Tel: 86-755-8864-2200

China - Suzhou
Tel: 86-186-6233-1526

China - Wuhan
Tel: 86-27-5980-5300

China - Xian
Tel: 86-29-8833-7252

China - Xiamen
Tel: 86-592-2388138

China - Zhuhai
Tel: 86-756-3210040

ASIA/PACIFIC

India - Bangalore
Tel: 91-80-3090-4444

India - New Delhi
Tel: 91-11-4160-8631

India - Pune
Tel: 91-20-4121-0141

Japan - Osaka
Tel: 81-6-6152-7160

Japan - Tokyo
Tel: 81-3-6880-3770

Korea - Daegu
Tel: 82-53-744-4301

Korea - Seoul
Tel: 82-2-554-7200

Malaysia - Kuala Lumpur
Tel: 60-3-7651-7906

Malaysia - Penang
Tel: 60-4-227-8870

Philippines - Manila
Tel: 63-2-634-9065

Singapore
Tel: 65-6334-8870

Taiwan - Hsin Chu
Tel: 886-3-577-8366

Taiwan - Kaohsiung
Tel: 886-7-213-7830

Taiwan - Taipei
Tel: 886-2-2508-8600

Thailand - Bangkok
Tel: 66-2-694-1351

Vietnam - Ho Chi Minh
Tel: 84-28-5448-2100

EUROPE

Austria - Wels
Tel: 43-7242-2244-39
Fax: 43-7242-2244-393

Denmark - Copenhagen
Tel: 45-4485-5910
Fax: 45-4485-2829

Finland - Espoo
Tel: 358-9-4520-820

France - Paris
Tel: 33-1-69-53-63-20
Fax: 33-1-69-30-90-79

Germany - Garching
Tel: 49-8931-9700

Germany - Haan
Tel: 49-2129-3766400

Germany - Heilbronn
Tel: 49-7131-72400

Germany - Karlsruhe
Tel: 49-721-625370

Germany - Munich
Tel: 49-89-627-144-0
Fax: 49-89-627-144-44

Germany - Rosenheim
Tel: 49-8031-354-560

Israel - Ra'anana
Tel: 972-9-744-7705

Italy - Milan
Tel: 39-0331-742611
Fax: 39-0331-466781

Italy - Padova
Tel: 39-049-7625286

Netherlands - Drunen
Tel: 31-416-690399
Fax: 31-416-690340

Norway - Trondheim
Tel: 47-7288-4388

Poland - Warsaw
Tel: 48-22-3325737

Romania - Bucharest
Tel: 40-21-407-87-50

Spain - Madrid
Tel: 34-91-708-08-90
Fax: 34-91-708-08-91

Sweden - Gothenberg
Tel: 46-31-704-60-40

Sweden - Stockholm
Tel: 46-8-5090-4654

UK - Wokingham
Tel: 44-118-921-5800
Fax: 44-118-921-5820